Earth Syst. Dynam. Discuss., https://doi.org/10.5194/esd-2019-7
Manuscript under review for journal Earth Syst. Dynam.
Discussion started: 28 February 2019

Earth System Dynamics Discussions
Open Access

A climatological interpretation of precipitation-based $\delta^{18}O$ across Siberia and Central Asia

Tao Wang [a, b], Ting-Yong Li [a, b, *], Jian Zhang [a, b], Yao Wu [a, b], Chao-Jun Chen [a, b], Ran Huang [a, b], Jun-Yun Li [a, b], Si-Ya Xiao [a, b]

[a] *Chongqing Key Laboratory of Karst Environment, School of Geographical Sciences, Southwest University, Chongqing 400715, China*

[b] *Field Scientific Observation & Research Base of Karst Eco-environments at Nanchuan in Chongqing, Ministry of Nature Resources of China, Chongqing 408435, China*

*** The corresponding author:**

Ting-Yong Li,

E-mail: cdlty@swu.edu.cn;

Tel: (O) +86-23-68367170; Mobile: +86-13637907815

Postal Address: No. 2 Tiansheng Road, Beibei district, Chongqing, P.R. China, 400715. School of Geographical Sciences, Southwest University.

Earth Syst. Dynam. Discuss., https://doi.org/10.5194/esd-2019-7
Manuscript under review for journal Earth Syst. Dynam.
Discussion started: 28 February 2019

Abstract

Siberia and Central Asia are located at mid- to high latitudes and encompass a large landlocked area of the Eurasian continent containing vast tracts of permafrost (seasonal permafrost and permafrost), which is extremely sensitive to global climate change. However, previous research has scarcely investigated the changes in the paleoclimate in this region. Similarly, the temporal and spatial distributions of the stable isotopic composition ($\delta^{18}O_P$) of precipitation and its corresponding influencing factors remain largely unknown. Therefore, we used data from 15 Global Network of Isotopes in Precipitation (GNIP) stations to investigate the relationships between $\delta^{18}O_P$ and the local temperature and precipitation considering changes in atmospheric circulation. Analyses conducted on the monthly, seasonal and annual timescales led to three main conclusions. **(1)** At the monthly timescale, the variations in $\delta^{18}O_P$ exhibited a significant positive correlation with the monthly mean temperature ($p < 0.01$). The $\delta^{18}O_P$ excursion was positive in summer as the temperature increased and negative in winter as the temperature decreased. Note that the $\delta^{18}O_P$ values were also affected by the monthly precipitation, Eurasian zonal circulation index (EZCI), and water vapor source (e.g., polar air masses and local evaporative water vapor). **(2)** At the annual scale, the weighted average value of the precipitation-based $\delta^{18}O$ ($\delta^{18}O_w$) exhibited a "temperature effect" over 60 °N – 70 °N. However, $\delta^{18}O_w$ may have been dominated by multiple factors from 40 °N to 60 °N (e.g., the North Atlantic Oscillation (NAO) and water vapor source changes). **(3)** At the annual timescale, the variability of the path of the westerly caused by changes in the NAO explained the variations in both $\delta^{18}O_P$ and

Earth Syst. Dynam. Discuss., https://doi.org/10.5194/esd-2019-7
Manuscript under review for journal Earth Syst. Dynam.
Discussion started: 28 February 2019

Earth System Dynamics Open Access Discussions

$\delta^{18}O_W$.

Based on the limited observational data in this region, we found that $\delta^{18}O_P$ is correlated with the local temperature at the monthly and seasonal timescales. However, at the annual timescale, in addition to the temperature effect, $\delta^{18}O_P$ reflects the variability of the water vapor source that is dominated by the EZCI and NAO. Therefore, it is possible to reconstruct the histories of past atmospheric circulations and water vapor sources in this region via geologic $\delta^{18}O$ proxies, e.g., speleothems records.

Keywords: Siberia and Central Asia, $\delta^{18}O_p$, Eurasian Zonal Circulation, North Atlantic Oscillation, Moisture sources

1. Introduction

The stable oxygen isotopic compositions ($\delta^{18}O$) of ice cores, tree rings, ocean sediments and cave speleothems have been widely used as proxies for paleoclimatic change; however, the meaning of $\delta^{18}O$ varies among different paleo-archives and hence remains controversial (Wang et al., 2001). Therefore, monitoring the $\delta^{18}O$ of modern atmospheric precipitation ($\delta^{18}O_P$) can lead to a better understanding of the climatic significance of $\delta^{18}O$ in various paleo-archives.

The Global Network of Isotopes in Precipitation (GNIP) became operational in 1961 when it was established by the World Meteorological Organization (WMO) and the International Atomic Energy Agency (IAEA); through the GNIP, stable hydrogen and oxygen isotopic compositions of precipitation (δD and $\delta^{18}O_P$) were first observed, thereby providing numerous isotope data sets for research on global and local atmospheric circulation (Rozanski et al., 1993). Subsequent related studies have indicated that the factors influencing the changes in δD and $\delta^{18}O_P$ exhibit distinct characteristics at different latitudes, e.g., the variations in $\delta^{18}O_P$ over mid- and high-latitude regions are dominated by the temperature, while those at low latitudes are dominated by precipitation (Dansgaard, 1964; Rozanski et al., 1992; Hoffmann and Heimann, 1997; Aragufis-Aragufis et al., 1998; Yamanaka et al., 2007; Tang et al., 2015). In addition, changes in the source of water vapor and in the atmospheric circulation pattern can also result in variations in δD and $\delta^{18}O_P$ (Cruz Jr et al., 2005; Krklec et al., 2018).

Siberian permafrost constitutes one of the most important forms of tundra in the world and acts as an indicator of temperature change; accordingly, the greenhouse gases released through the melting of permafrost have important impacts on global climate change and carbon cycle processes (Dobinski, 2011; Schuur et al., 2015; Raudina et al., 2018). However, modern meteorological monitoring networks and paleoclimatic research are relatively scarce in Siberia and northern Central Asia in comparison with other regions worldwide. Consequently, the findings of previous research on the stable isotopes of precipitation in this region can be summarized as follows. (1) The stable isotopes of meteoric precipitation are controlled by the local temperature with a distinct "temperature effect" (Kurita et al., 2004; Yu et al., 2016). (2) The main source of moisture in Eurasia originates from the Atlantic Ocean (Aizen et al., 1996; Numaguti, 1999). While, throughout the summer season, the supply of circulating water is an

Earth Syst. Dynam. Discuss., https://doi.org/10.5194/esd-2019-7
Manuscript under review for journal Earth Syst. Dynam.
Discussion started: 28 February 2019

important contribution. Additionally, isotopic changes in circulating water also affect the relationship between $\delta^{18}O_P$ and temperature (Kurita et al., 2004; Aizen et al., 2005; Henderson et al., 2006; Butzin et al., 2014; Wolff et al., 2016). (3) The zonal index (ZI) represents the intensity of the mid-latitude westerly wind, a common circulation pattern that leads to changes in the transport of water vapor over Siberia and central Asia. Moreover, the variation in $\delta^{18}O_P$ is positively correlated with the frequency of the westerly wind (Kurita, 2003; Li and Wang, 2003; Aizen et al., 2005; Yu et al., 2016). (4) The climate of western Siberia displays strong interannual variations that are dominated by the North Atlantic Oscillation (NAO) during the winter period (Peng and Mysak, 1993; Zhao et al., 2011; Casado et al., 2013; Butzin et al., 2014; Wolff et al., 2016). The regional temperature also affects the decadal winter variations in $\delta^{18}O_P$, but the interannual summer variations in $\delta^{18}O_P$ can be attributed to short-term regional scale processes, such as evaporation and convective precipitation (Casado et al., 2013; Butzin et al., 2014).

Therefore, the $\delta^{18}O_P$ distribution in Siberia may be controlled either by the temperature effect or by variations in the source of water vapor. Nevertheless, some scientific questions remain that are worthy of further study. Notably, how do the abovementioned factors affect the isotopic composition of local atmospheric precipitation at different timescales (e.g., monthly, seasonal and annual)? In addition, the NAO has an enormous influence on the climate patterns at mid- to high latitudes within the Northern Hemisphere (Hurrell et al., 2003; Casado et al., 2013). Notably, monitoring data, climate simulation results, and paleoclimate proxies from Europe highlight a strong relationship between $\delta^{18}O_P$ and the North Atlantic Oscillation index (NAOI) (Baldini et al., 2008; Field, 2010; Sidorova et al., 2010; Mischel et al., 2015; Wassenburg et al., 2016). However, whether signals associated with the NAO can be recorded in the Siberian $\delta^{18}O_P$ remains unknown; similarly, the influences of Atlantic water vapor and Arctic Ocean water vapor on the regional precipitation are poorly understood. Consequently, analyses of the abovementioned scientific problems will provide more in-depth comprehension of the climatic and environmental significance of the isotopic composition of atmospheric precipitation throughout the region. Moreover, a thorough understanding of the physical mechanisms related to regional changes in modern meteoric isotopes will provide a framework for reconstructing the regional paleoclimate via geological records, such as speleothems and ice core records.

In this paper, we analyzed stable isotopic observation data pertaining to atmospheric precipitation at 15 GNIP sites over Siberia and northern Central Asia (40 °N – 70 °N, 50 °E – 120 °E) (Fig. 1). By combining these data with observed changes in the patterns of atmospheric circulation, we investigated the following scientific issues: (1) the variations in the characteristics of atmospheric precipitation isotopes in Siberia and their influencing factors at monthly, seasonal and annual timescales; (2) the relationship between the isotopic compositions of precipitation and atmospheric circulations in Siberia; and (3) the main factors associated with the stable isotopic composition of atmospheric precipitation in this region and their climatic and environmental significance. These topics were then analyzed and discussed to provide reliable support for modern monitoring endeavors, thereby facilitating paleoclimatic

Earth Syst. Dynam. Discuss., https://doi.org/10.5194/esd-2019-7
Manuscript under review for journal Earth Syst. Dynam.
Discussion started: 28 February 2019

reconstruction efforts via regional $\delta^{18}O$ proxies.

2. Study area

The study region, which is located in the northern part of Eurasia, includes inland Siberia and the northern part of Central Asia (40 °N – 70 °N, 50 °E – 120 °E) (Fig. 1). The region of interest herein is a typical mid- to high-latitude continental area extending from the Ural Mountains in the west to the Stanovoy Range in the east and from the Arctic Ocean in the north to a series of mountain ranges toward the south, namely, the mountains in northern Kazakhstan to the southwest, Urumqi in the south, and Qiqihar (northeastern China) to the southeast.

The moisture over Eurasia is transported by the westerly, and the water vapor flux decreases as the wind direction shifts from West Eurasia to East Eurasia (Aizen et al., 1996; Numaguti, 1999; Kurita et al., 2004; Wang et al., 2017). The elevations of the sites in the study region range from 53 to 1338 m a.s.l. (above sea level), the annual average temperature varies from -11.8 to 10.0 ℃, and the annual average precipitation reaches 230 – 706 mm (Table 1). In winter, the precipitation in this region originates from the ocean, whereas half of the precipitation in summer is sourced from the local evaporation of water vapor due to the high evaporation rate (Numaguti, 1999; Kurita et al., 2004; Butzin et al., 2014). In autumn and winter, the climatic conditions in this region are controlled mainly by the Siberian high-pressure system; the surface evaporation within the study area is relatively weak during these seasons due to the low temperature and high snow cover, resulting in a wide range of cold and dry conditions throughout Siberia (Henderson et al., 2006).

3. Data and methods

The meteoric isotopic and meteorological data in this paper were derived from the GNIP. We used atmospheric stable isotopic observation data from 15 stations located in the study region for statistical analysis. Twelve of the stations (i.e., except for those in Ulaanbaatar, Wulumuqi, and Qiqihar) are located in Russia (Fig. 1; Table 1). We further collected synchronous data from 14 other sites in Eurasia outside the study area to support the discussion (Fig. 1). The $\delta^{18}O_p$ data were downloaded through the IAEA website (https://nucleus.iaea.org/wiser/index.aspx/). The monitoring period ranged from 1961 to 2015; within this period, the data for some years were missing. The NAOI data were downloaded from the National Centers for Environmental Prediction (NCEP) of the National Oceanic and Atmospheric Administration (NOAA) (http://www.cpc.ncep.noaa.gov/data/indices/). The Eurasian zonal circulation index (EZCI) data were downloaded from the National Climate Center of the China Meteorological Administration (http://cmdp.ncc-cma.net/cn/monitoring.htm).

To identify the moisture transport paths and better interpret the $\delta^{18}O_P$ variability at different sites, we determined the back trajectories of air parcels using the NCEP reanalysis data sets (ftp://arlftp.arlhq.noaa.gov/pub/archives/reanalysis) and the Hybrid Single-Particle Lagrangian Integrated Trajectory (HYSPLIT) model, which is available from the NOAA Air Resources Laboratory at http://ready.arl.noaa.gov/HYSPLIT.php

We compared the results for the identified moisture sources at four different

Earth Syst. Dynam. Discuss., https://doi.org/10.5194/esd-2019-7
Manuscript under review for journal Earth Syst. Dynam.
Discussion started: 28 February 2019

elevations, namely, 500, 1000, 1500 and 2000 m a.g.l. (above ground level), for four sites: Bagdarin, Qiqihar, Ulaanbaatar and Wulumuqi. Most of the moisture in the atmosphere is believed to reside up to 2000 m a.g.l. (Zhang, 2009; Bershaw et al., 2012; Yu et al., 2016; Krklec et al., 2018); therefore, no higher levels were considered. The results revealed little variation in the sources of moisture at different elevations (Appendix Fig. 1 - 3) (Krklec and Domínguez-Villar, 2014). Hence, the air mass history was calculated for a single elevation of 1000 m a.g.l. during the previous 240-h (10-day) period, which is considered the average residence time of water vapor in the atmosphere (Numaguti, 1999; Krklec and Domínguez-Villar, 2014; Krklec et al., 2018).

4. Results

4.1 Seasonal variations in $\delta^{18}O_P$ and *d-excess*

Six monitoring sites that recorded over two years of continuous $\delta^{18}O_P$ data, namely, Amderma, Pechora, Perm, Salekhard, Qiqihar and Wulumuqi, were selected to analyze the seasonal variations in $\delta^{18}O_P$. The average monthly temperature and $\delta^{18}O_P$ exhibited synchronous seasonal variations; specifically, $\delta^{18}O_P$ displayed positive excursions in summer and negative excursions in winter, while the maximum average monthly temperature appeared in July, and the minimum average monthly temperature was observed in January. The $\delta^{18}O_P$ extrema followed a similar trend: the maximum values occurred in July, while the minimum values occurred between December and February (Fig. 2).

An analysis of the seasonal changes in the deuterium excess (*d-excess*) at these six

Earth Syst. Dynam. Discuss., https://doi.org/10.5194/esd-2019-7
Manuscript under review for journal Earth Syst. Dynam.
Discussion started: 28 February 2019

Earth System Dynamics
Open Access
Discussions

monitoring sites indicated that *d-excess* at Wulumuqi displayed obvious seasonal variations. In contrast, no obvious seasonal changes were observed for *d-excess* either at Qiqihar in East Asia or at Amderma, Pechora, Perm, or Salekhard in northern Siberia (Fig. 3).

4.2 Relationship between δD and $\delta^{18}O_P$

Craig (1961) used the relationship between δD and $\delta^{18}O_P$ to establish the first global meteoric water line (GMWL): $\delta D = 8.0\ \delta^{18}O + 10.0$ (Craig, 1961); in the GMWL, the slope reflects the fractionation or ratio between δD and $\delta^{18}O_P$, while the intercept indicates the extent to which δD deviates from equilibrium (Craig, 1961). As shown in Fig. 4, a correlation analysis was performed on the relationship between δD and $\delta^{18}O_P$ with data from the 15 stations in Siberia and Central Asia to obtain the local meteoric water line (LMWL): $\delta D = 7.8\ \delta^{18}O + 5.0$ ($R = 0.98$). We used the δD and $\delta^{18}O_P$ data from monthly precipitation observations collected at every GNIP site to obtain the LMWL equations given in Table 2.

The LMWL slopes were generally lower than the GMWL slope at all 15 stations (except for Novosibirsk, Irkutsk, Enisejsk and Perm) (Table 2). As a result of evaporation during the precipitation period in the inland region, the enrichment of $\delta^{18}O_P$ led to equations for atmospheric precipitation with a lower slope at most monitoring sites (Dansgaard, 1964; Stewart, 1975; Peng et al., 2005; Yamanaka et al., 2007; Pang et al., 2011; Chen et al., 2015). The differences in the LMWL among the various sites in the study region may be attributed to differences in source of water vapor. However,

Earth Syst. Dynam. Discuss., https://doi.org/10.5194/esd-2019-7
Manuscript under review for journal Earth Syst. Dynam.
Discussion started: 28 February 2019

the observed continental characteristics generally exhibited low slope and low intercept values, as presented in Table 2 (Stewart, 1975; Peng et al., 2005; Peng et al., 2007; Chen et al., 2015).

4.3 Relationship between temperature and $\delta^{18}O_p$

4.3.1. Relationship between the monthly average temperature and $\delta^{18}O_P$

The correlation coefficients between $\delta^{18}O_P$ and monthly average temperature are summarized in Table 3 for 13 stations that recorded at least one full year of $\delta^{18}O_P$ data during the observation period. A significant positive correlation was found between $\delta^{18}O_P$ and the monthly average temperature (Table 3) with an obvious temperature effect (Dansgaard, 1964).

According to the patterns of changes in the multiyear temperature and precipitation records, a year is divided into four seasons: spring (March–April−May, MAM), summer (June−July–August, JJA), autumn (September−October–November, SON), and winter (December−January–February of the following year, DJF) (Kurita et al., 2004). We analyzed the correlation between $\delta^{18}O_P$ and the monthly average temperature in every season at every site that recorded $\delta^{18}O_P$ data for at least two years (Table 3). Based on the results, the correlation between $\delta^{18}O_P$ and the monthly average temperature in spring and autumn is more significant than that in winter and summer, thereby demonstrating the dominant effect of temperature in the former (Table 3). The correlation between $\delta^{18}O_P$ and the monthly average temperature was weakest in summer, demonstrating that the effect of temperature on $\delta^{18}O_P$ is relatively imperceptible during this season. This result may be attributed to the strong surface water evaporation in summer, during which more than 80% of all precipitation in Eurasia originates from surface evaporation; notably, a large portion of water evaporated from the surface comes from winter precipitation, which has smaller $\delta^{18}O_P$ values than does summer precipitation, leading to the low correlation between $\delta^{18}O_P$ and temperature in the summer season (Numaguti, 1999; Kurita et al., 2004; Henderson et al., 2006).

In addition, Kurita et al. (2003) noted that the isotope composition of meteoric precipitation in eastern Siberia is controlled by Rayleigh fractionation in spring and by water vapor transported by the westerly with relatively high $\delta^{18}O_P$ values in summer; this water vapor may also be mixed with snowmelt water characterized by a low $\delta^{18}O_P$ value. Therefore, the temperature effect of $\delta^{18}O_P$ is not evident because of the influence of changes in the source of water vapor in summer (Kurita, 2003; Blyakharchuk et al., 2007).

4.3.2. The relationship between the annual average temperature and $\delta^{18}O_W$

A correlation analysis was conducted between the weighted mean $\delta^{18}O$ in annual precipitation ($\delta^{18}O_W$) and the annual average temperature at 20 stations that recorded over 5 years of $\delta^{18}O_P$ data. The $\delta^{18}O_W$ values at Espoo, Krakow, Kuopio and Salekhard exhibited a significant positive correlation ($p < 0.05$) with the average annual temperature; however, either no significant positive correlation or a weak negative correlation was observed at the other stations (Table 4).

The stations north of 60 °N exhibited a positive correlation between the annual average temperature and $\delta^{18}O_P$; in contrast, the correlation coefficient (R) was irregular at the sites south of 60 °N. Therefore, we propose that the distribution of $\delta^{18}O_W$ at high latitudes over Eurasia reflects the changes in the annual average temperature, while the $\delta^{18}O_W$ distribution in the range of 40 °N – 60 °N does not follow temperature trend at the interannual scale. For example, the correlation coefficient (R) between $\delta^{18}O_W$ and the annual average temperature at Qiqihar was negative, which is attributed to the proximity of the site to the Pacific Ocean and the effect of the Asian summer monsoon (Li et al., 2012b). Moreover, Wulumuqi displayed a negative correlation coefficient (R) between $\delta^{18}O_W$ and the annual average temperature due to the north-south swinging of the westerly wind at the interannual scale (Liu et al., 2015). Therefore, the annual mean temperature and $\delta^{18}O_W$ exhibited a temperature effect at high latitudes (60 °N – 70 °N). However, at an annual scale, the regions located within 40 °N – 60 °N may be situated in a transition zone of the temperature effect in addition to a “rainfall effect” and a “circulation effect”. Therefore, different monitoring sites are characterized by different controlling factors, resulting in varying relationships between $\delta^{18}O_P$ and the annual average temperature (Rozanski et al., 1992; Johnson and Ingram, 2004; Krklec and Domínguez-Villar, 2014; Wang et al., 2017; Li, 2018; Zhang and Li, 2018).

4.4. Relationship between precipitation and $\delta^{18}O_p$

We analyzed the correlation between $\delta^{18}O_P$ and the monthly precipitation at 13

Earth Syst. Dynam. Discuss., https://doi.org/10.5194/esd-2019-7
Manuscript under review for journal Earth Syst. Dynam.
Discussion started: 28 February 2019

Earth System Dynamics Discussions Open Access EGU

sites that recorded more than one year of $\delta^{18}O_P$ data (12 months/year). A significant positive correlation was observed between $\delta^{18}O_P$ and the monthly precipitation at most sites (Table 5); furthermore, the correlation coefficient between $\delta^{18}O_P$ and the monthly precipitation (R_P) at every station (Table 5) was less than that between $\delta^{18}O_p$ and the monthly average temperature (R_T) (Table 3). Because $\delta^{18}O_P$ is controlled by the temperature distribution in the study region at the monthly timescale (Table 3), a significant correlation exists between the monthly average temperature and monthly precipitation at each monitoring site (Appendix Table 1), resulting in a positive correlation between $\delta^{18}O_P$ and the monthly precipitation (Table 5). At the annual timescale, the positive correlation between $\delta^{18}O_P$ and the monthly precipitation is contrary to the general rainfall effect. In every season, the relationship between the monthly precipitation and monthly $\delta^{18}O_P$ displays a negative correlation, which seems to be consistent with the rainfall effect (Dansgaard, 1964), although this negative correlation is not very significant (Table 5).

Most of the monitoring stations (14 out of 20) that recorded over 5 years of data exhibited a nonsignificant negative relationship between $\delta^{18}O_W$ and the annual precipitation amount (Table 4). This lack of significance may be due to the limited amount of observation data. Nevertheless, based on the limited observational data available, we can make a preliminary judgment insomuch that the precipitation amount at the interannual scale may not principally influence the $\delta^{18}O_W$ values of the mid- to high-latitude regions of Eurasia.

5. Discussion

5.1. *d-excess* was used to represent a source of water vapor

Diagnosing nonequilibrium fractionation requires an analysis of *d-excess* (measured in ‰), which is defined as *d-excess* = δD - 8δ^{18}O (Dansgaard, 1964). Related studies have shown that *d-excess* is influenced primarily by the relative humidity of the water vapor source when an air mass forms. When the relative humidity of the water vapor source is low, the corresponding *d-excess* value is high, and vice versa. Based on these findings, *d-excess* reflects the thermal conditions and the water vapor balance when an air mass forms, and thus, *d-excess* has been widely used to track the source of precipitation (Pfahl and Wernli, 2008; Pfahl and Sodemann, 2014; Krklec et al., 2018).

Six observation sites that recorded $\delta^{18}O_P$ data continuously for at least two years, namely, Amderma, Pechora, Perm, Salekhard, Qiqihar, Wulumuqi, were selected to analyze the seasonal variations in *d-excess* in atmospheric precipitation (Fig. 3). Specifically, *d-excess* exhibits obvious seasonal variations at Wulumuqi, where the winter *d-excess* distribution is higher than average, and the summer (JJA) *d-excess* distribution is lower than average. In contrast, the regional *d-excess* distribution is lower in summer as a result of the low temperature and high humidity associated with Atlantic moisture from the northwest (Fig. 5C). Meanwhile, in winter (DJF), warm and dry water vapor originating from the southwestern Black Sea, Caspian Sea and Aral Sea lead to an increase in *d-excess* (Fig. 5) (Tian et al., 2007; Li et al., 2012a). Aizen et al. (2005) investigated ice core and snowfall records from the Altai region (northern Wulumuqi (49 °N – 50 °N, 86 °E – 88 °E)) and found two distinct moisture sources: oceanic sources from the Atlantic Ocean and the Arctic Ocean with *d-excess* < 12‰

Earth Syst. Dynam. Discuss., https://doi.org/10.5194/esd-2019-7
Manuscript under review for journal Earth Syst. Dynam.
Discussion started: 28 February 2019

Earth System Dynamics
Discussions
Open Access

and an inland evaporative mass from the Aral Sea and the Caspian Sea with *d-excess* > 12‰. Based on the above analysis, the seasonal variation in *d-excess* in the precipitation over Wulumuqi is controlled by different moisture sources (Fig. 5).

There are no significant seasonal variations in the *d-excess* of the precipitation over East Asia (Qiqihar) and Northwest Siberia (Amderma, Pechora, Perm and Salekhard) (Fig. 3A - 3E). This finding may be attributed to the moisture transport mechanisms of different regions. For example, because they are located farther to the north, Amderma, Pechora, Perm, and Salekhard are more susceptible to moisture originating from the Arctic Ocean (Tian et al., 2007). Additionally, Qiqihar is influenced by moisture from the Atlantic and Arctic Oceans transported by westerly winds, and the local precipitation is further affected by moisture from the Pacific Ocean transported by the East Asian summer monsoon (Li et al., 2012b).

The *d-excess* value reflects not only the characteristics of the water vapor source temperature, relative humidity, and evaporation strength but also the secondary evaporation of raindrops during their descent from the clouds to the ground (Peng et al., 2005; Pfahl and Sodemann, 2014; Chen et al., 2015). In the annual precipitation at Wulumuqi, the *d-excess* values vary between -16.7‰ and 54.8‰ with an average value of 13.3‰, which is higher than the global *d-excess* average (approximately 10‰). The *d-excess* value obtained in the precipitation over Wulumuqi is similar to that obtained over the Mediterranean region, where a secondary evaporation effect is produced below the clouds, reflecting the local dry climate conditions (Peng et al., 2005; Hou et al., 2011; Wang et al., 2016).

Earth Syst. Dynam. Discuss., https://doi.org/10.5194/esd-2019-7
Manuscript under review for journal Earth Syst. Dynam.
Discussion started: 28 February 2019

5.2. Relationship between the EZCI and $\delta^{18}O_P$

The EZCI was used to represent the variation in the intensity of the westerly. When the zonal circulation became strengthened (weakened) during the winter season, the westerly became strengthened (weakened) as the intensity of the warm oceanic air mass from the Atlantic increased (decreased) and the intensity of the cold continental air mass decreased (increased), resulting in rising (falling) winter temperatures over Europe and northern Asia. In contrast, when the zonal circulation became strengthened (weakened) during the summer period, the westerly winds became strengthened (weakened), the intensity of the cool air mass from the Atlantic Ocean increased (decreased), and the intensity of the warm air mass from the continent decreased (increased), resulting in a decrease (increase) in the summer temperatures over Europe and northern Asia (Li and Wang, 2003; Hoy et al., 2012; Nowosad, 2017). Our results show that the monthly $\delta^{18}O_P$ values at most stations (9 out of 13) exhibit a significant negative correlation with the EZCI (Table 6). At the seasonal timescale, at most sites, the two variables exhibit a positive correlation in winter and a negative correlation in spring and autumn. In summer, only the Pechora site displays a significant negative correlation between the EZCI and $\delta^{18}O_P$ (Table 5).

At the annual and seasonal timescales, the different correlations between $\delta^{18}O_P$ and the EZCI are the result of seasonal variations in the temperature and zonal wind. At the annual timescale, the EZCI displays seasonal variations that are opposite to those of the temperature (the EZCI is high in winter and low in summer) (Appendix Fig. 4); additionally, $\delta^{18}O_P$ and the monthly average temperature are positively correlated at the

Earth Syst. Dynam. Discuss., https://doi.org/10.5194/esd-2019-7
Manuscript under review for journal Earth Syst. Dynam.
Discussion started: 28 February 2019

annual timescale (Table 3), resulting in a significant negative correlation between $\delta^{18}O_P$ and the EZCI. In winter, when the zonal circulation is stronger (weaker), the westerly wind becomes strengthened (weakened), and the temperatures over Europe and northern Asia increase (decrease); therefore, there is a positive correlation between $\delta^{18}O_P$ and the EZCI in winter. In contrast, in spring and autumn, a negative correlation is found between $\delta^{18}O_P$ and the EZCI due to the increase (decrease) in the intensity of the westerly wind, and this correlation leads to a decrease (increase) in the temperature and $\delta^{18}O_P$ value (Hoy et al., 2012). In summer, as the EZCI weakens (Appendix Fig. 4), the Arctic vortex extends toward the south (Hoy et al., 2012), and the mixing of water vapor from the Arctic and Pacific Oceans with inland local evaporative water influences the relationship among the EZCI, $\delta^{18}O_P$, and temperature; therefore, the correlation coefficient (R) between $\delta^{18}O_P$ and the EZCI varies at each site. For example, in July 1996 and July 1998, the temperatures at Bagdarin were similar (16.9 and 16.8 °C, respectively), whereas the $\delta^{18}O_P$ values were quite different (-10.3 and -15.8 (‰, V-SMOW), respectively). This difference can be attributed to the increase in moisture originating from the Pacific Ocean in July 1996, leading to a positive $\delta^{18}O_P$ value (Fig. 6A, 6B). Furthermore, the temperature at Qiqihar was 6.2 °C in April 1990 and April 1991; the increase in water vapor from the Arctic Ocean led a lower $\delta^{18}O_P$ value in April 1990 (-18.0 (‰, V-SMOW)) than in April 1991 (-16.2 (‰, V-SMOW)) (Fig. 6C, 6D). In both July 1994 and August 2000, the temperature at Ulaanbaatar was 17.1 °C, the $\delta^{18}O_P$ values were -4.0 and -10.4 (‰, V-SMOW), respectively (Fig. 6E, 6F), and the EZCI values were 6.1 and 10.9, respectively. In July 1994, the EZCI decreased as the westerly wind weakened, in which inland evaporation played a leading role (Fig. 6E). Moreover, warm water vapor from South China also affected the precipitation in the region and led to the enrichment of $\delta^{18}O_P$ in July 1994 (Fig. 6E). Conversely, in 2000, almost all water vapor originated from high-latitude areas (the high latitudes of the North Atlantic and near the Ural Mountains), and the $\delta^{18}O_P$ values were low (Fig. 6F). Finally, in July and August 2001, the temperature at Wulumuqi was 23.4 °C, and the EZCI (6.8) in July was lower than that in August (10.3). The polar air mass invaded Wulumuqi in July, resulting in a lower $\delta^{18}O_P$ value (-7.4 (‰, V-SMOW)) than that in August (-3.9 (‰, V-SMOW)) (Fig. 6G, 6H).

The above results suggest that changes in the moisture sources and their relative proportions caused by variations in zonal circulation explain not only the complex correlation between the EZCI and $\delta^{18}O_P$ in summer but also why the temperature effect in summer is less obvious than that in spring and autumn.

5.3. Relationship between the NAO and $\delta^{18}O_P$

From 1980 to 1983, the sites with continuous records, namely, Amderma, Arkhangelsk, Kalinin, Pechora, Perm, Riga, and St. Petersburg, were selected to analyze the $\delta^{18}O_P$ trends at different sites during this period. With the exception of Riga, negative $\delta^{18}O_P$ trends were found for all the other stations, contrary to the trends for the NAO and EZCI (Fig. S5). We removed Riga and Amderma, which had missing data, from the data set and arithmeticlly averaged and combined the $\delta^{18}O_P$ time series from Arkhangelsk, Kalinin, Pechora, Perm and St. Petersburg (Fig. 7A) into a single $\delta^{18}O_P$

sequence (Fig. 7B). Additionally, the NAOI and EZCI were compared with the $\delta^{18}O_P$ sequence (Fig. 7C, 7D). Evident fluctuations can be observed in the $\delta^{18}O_P$, NAOI and EZCI curves, which exhibit opposing trends (Fig. 7B, 7C, 7D). Taking 1981 (NAOI: -0.21) and 1982 (NAOI: 0.43) as examples for comparison, when the NAO is negative (1981), the westerly wind shifts southward (~ 45 °N – 55 °N), bringing warmer water vapor from the southwest to the northeast and resulting in higher $\delta^{18}O_W$ values (Fig. 8A). When the NAO is positive (1982), the westerly strengthens, migrates toward the north (~ 50 °N – 60 °N) and generally moves in the zonal direction; therefore, the $\delta^{18}O_W$ values will be relatively small (Fig. 8B). The NAO influences the changes in both $\delta^{18}O_P$ and $\delta^{18}O_W$ by affecting the intensity and pathway of the westerly (Hurrell, 1995; Field, 2010; Langebroek et al., 2011). Therefore, we speculate that over mid- to high-latitude regions throughout Eurasia, $\delta^{18}O_W$ is affected by both the NAO and the temperature. This joint influence is the main reason for the absence of a temperature effect in the variability of $\delta^{18}O_W$ at the interannual time scale.

6. Conclusions

This paper selected 15 GNIP stations situated throughout Siberia and Central Asia for analysis in combination with the changes in atmospheric circulation patterns at mid- to high latitudes; the conclusions of this study are as follows.

(1) At the monthly and seasonal time scales, the summer $\delta^{18}O_P$ values were high, and the winter $\delta^{18}O_P$ values were small, thereby exhibiting a “temperature effect”. At the annual time scale, the average temperature and $\delta^{18}O_W$ exhibited a temperature effect

at high latitudes (60 °N – 70 °N), but a significant temperature effect was not observed in regions over 40 °N – 60 °N.

(2) The $\delta^{18}O_P$ values were significantly positively correlated with the monthly precipitation at the monthly time scale, which is contrary to the general "rainfall effect". The above phenomenon is attributed to the similar seasonal change between the monthly average temperature and monthly precipitation in the study area. In comparison, no significant correlation was observed between either $\delta^{18}O_P$ or $\delta^{18}O_W$ and the local precipitation.

(3) The $\delta^{18}O_P$ values were negatively correlated with the EZCI at the monthly time scale. The zonal circulation results in changes in $\delta^{18}O_P$ throughout Eurasia by affecting the local temperature and water vapor source. The relationship among $\delta^{18}O_P$, the temperature and the EZCI varies seasonally and is influenced by changes in the source of water vapor in summer.

(4) The $\delta^{18}O_P$ values in the study region and the NAOI exhibit opposing trends at the interannual timescale. The NAO affects the source of water vapor transport by changing the pathways of the westerly, leading to changes in both $\delta^{18}O_P$ and $\delta^{18}O_W$.

In summary, the existing GNIP data compiled from meteoric isotope observations in Siberia and Central Asia are insufficient, particularly because the data records are not continuous. Based on these existing limited data, we speculate that the local atmospheric precipitation $\delta^{18}O_P$ is dominated by temperature at the monthly and seasonal timescales; at the interannual scale, the $\delta^{18}O_W$ variation is dominated by the

EZCI and NAO. Furthermore, there is no significant correlation between the annual average temperature or precipitation and $\delta^{18}O_W$. Therefore, reconstructing past atmospheric circulation patterns and changes in water vapor sources via $\delta^{18}O$ proxies (e.g., cave speleothems) in geologic archives within this region may be informative.

Acknowledgements

This research was supported by grants from the National Natural Science Foundation of China (NSFC; No. 41772170) and the Fundamental Research Funds for the Central Universities, China (Nos. XDJK2017A010 and XDJK2013A012) to T.-Y. Li.

Captions:

Fig. 1. Locations of the GNIP stations in Siberia and Central Asia (red triangles) and Europe (purple triangles) used in this study

Fig. 2. (A) Seasonal variations in $\delta^{18}O_P$ and (B) the monthly average temperature recorded at the GNIP stations in Siberia and Central Asia. The $\delta^{18}O_P$ values tend to be positive in summer and negative in winter, thereby exhibiting a "temperature effect".

Note: The sites that recorded $\delta^{18}O_P$ monitoring data for more than two years were selected, namely, Amderma, Pechora, Perm, Salekhard, Qiqihar, and Wulumuqi.

Fig. 3. Annual variations in *d-excess* at the GNIP stations in Siberia and Central Asia: (A) Amderma, (B) Pechora, (C) Perm, (D) Qiqihar, (E) Salekhard, and (F) Wulumuqi. The boxes represent the 25th–75th percentiles; the line through each box represents the

Earth Syst. Dynam. Discuss., https://doi.org/10.5194/esd-2019-7
Manuscript under review for journal Earth Syst. Dynam.
Discussion started: 28 February 2019

median; the whiskers indicate the 90th and 10th percentiles; and the points above and below the whiskers indicate the 95th and 5th percentiles. The *d-excess* pattern at Wulumuqi exhibited an obvious seasonal variation.

Note: The sites with $\delta^{18}O_P$ data for more than two years were selected, namely, Amderma, Pechora, Perm, Salekhard, Qiqihar, and Wulumuqi.

Fig. 4. LMWL (red line) based on the $\delta^{18}O$ and δD values (red dots) of precipitation from 15 stations in Central Asia and Siberia. The GMWL (blue line; Craig, 1961) is plotted for comparison.

Fig. 5. Seasonal mean moisture flux based on the NCEP/NOAA reanalysis data sets (1981–2010) integrated from 850 hPa. **(A)** DJF: December–January–February, **(B)** MAM: March–April–May, **(C)** JJA: June–July–August, and **(D)** SON: September–October–November. The vector in the figure is the water vapor transport q*v (unit: kg/(m*s)). The blue transparent bands indicate the main path of moisture transport for Wulumuqi (red triangle). In the Wulumuqi area, the moisture source in summer (JJA) is located more toward the north (from 50 °N to 60 °N, Atlantic Ocean), and the moisture sources in other seasons are more toward the southwest (from the Mediterranean Sea, Black Sea, and Caspian Sea).

Fig. 6. The back trajectories presented for Bagdarin **(A)** and **(B)**, Qiqihar **(C)** and **(D)**, Ulaanbaatar **(E)** and **(F),** and Wulumuqi **(E)** and **(F)** in different months. The bold black numbers in the figure are the monthly $\delta^{18}O_P$ values (‰, V-SMOW). The Hybrid Single-Particle Lagrangian Integrated Trajectory (HYSPLIT) model was used in the backward

Earth Syst. Dynam. Discuss., https://doi.org/10.5194/esd-2019-7
Manuscript under review for journal Earth Syst. Dynam.
Discussion started: 28 February 2019

Earth System Dynamics Discussions

tracking of air parcels for the above sites. The air mass history was calculated at 1000 m a.g.l. (above ground level) over the previous 240 h. Each dot represents the location of the air parcel at 12-h intervals. The model is available from the NOAA Air Resources Laboratory at http://ready.arl.noaa.gov/HYSPLIT.php. Months with similar average monthly temperatures but with significantly different $\delta^{18}O_P$ values were selected to compare the water vapor source. The changes in the water vapor source have an important influence on the variations in $\delta^{18}O_P$, as can be observed.

Fig. 7. Time series (1980-1983) of **(A)** $\delta^{18}O_P$ from Arkhangelsk (green dot), Kalinin (brown dot), Pechora (purple triangle), Perm (yellow triangle) and St. Petersburg (blue square). **(B)** Mean values of $\delta^{18}O_P$ from Arkhangelsk, Kalinin, Pechora, Perm and St. Petersburg. **(C)** NAOI and **(D)** EZCI. The dashed lines in **(B)**, **(C)** and **(D)** indicate the long-term trends.

Fig. 8. Spatial distribution of $\delta^{18}O_W$ values in the precipitation at the GNIP stations in different NAO phases. The circled numbers (1–6) indicate ① Riga, ② St. Petersburg, ③ Kalinin, ④ Arkhangelsk, ⑤ Perm, and ⑥ Pechora. The average atmospheric moisture transport moisture fluxes (vectors; unit: kg/ (m*s)) in different NAO phases are indicated: **(A)** 1981 (NAOI= -0.21) and **(B)** 1982 (NAOI= 0.43). The $\delta^{18}O_W$ values change due to different water vapor transport sources in different NAO phases.

Captions of the Appendix Figures

Appendix Fig. 1. The backward trajectories at Bagdarin **(A)** and **(B)**, Qiqihar **(C)** and

(D), Ulaanbaatar **(E)** and **(F)** and Wulumuqi **(E)** and **(F)** in different months. The bold black numbers in the figure are the monthly $\delta^{18}O_P$ values (‰, V-SMOW). The Hybrid Single-Particle Lagrangian Integrated Trajectory (HYSPLIT) model was used for the backward tracking of air parcels at the above sites. The air mass history was calculated at **500 m a.g.l.** (above ground level) over the previous 240 h. Each dot represents the location of the air parcel at 12-h intervals. The model is available from the NOAA Air Resources Laboratory at http://ready.arl.noaa.gov/HYSPLIT.php.

Appendix Fig. 2. The backward trajectories at Bagdarin **(A)** and **(B)**, Qiqihar **(C)** and **(D)**, Ulaanbaatar **(E)** and **(F)** and Wulumuqi **(E)** and **(F)** in different months. The bold black numbers in the figure are the monthly $\delta^{18}O_P$ values (‰, V-SMOW). The Hybrid Single-Particle Lagrangian Integrated Trajectory (HYSPLIT) model was used for the backward tracking of air parcels at the above sites. The air mass history was calculated at **1500 m a.g.l.** (above ground level) over the previous 240 h. Each dot represents the location of the air parcel at 12-h intervals. The model is available from the NOAA Air Resources Laboratory at http://ready.arl.noaa.gov/HYSPLIT.php.

Appendix Fig. 3. The backward trajectories at Bagdarin **(A)** and **(B)**, Qiqihar **(C)** and **(D)**, Ulaanbaatar **(E)** and **(F)** and Wulumuqi **(E)** and **(F)** in different months. The bold black numbers in the figure are the monthly $\delta^{18}O_P$ values (‰, V-SMOW). The Hybrid Single-Particle Lagrangian Integrated Trajectory (HYSPLIT) model was used for the backward tracking of air parcels at the above sites. The air mass history was calculated at **2000 m a.g.l.** (above ground level) over the previous 240 h. Each dot represents the location of the air parcel at 12-h intervals. The model is available from the NOAA Air

Earth Syst. Dynam. Discuss., https://doi.org/10.5194/esd-2019-7
Manuscript under review for journal Earth Syst. Dynam.
Discussion started: 28 February 2019

Earth System Dynamics Discussions

Resources Laboratory at http://ready.arl.noaa.gov/HYSPLIT.php.

Appendix Fig. 4. Annual variations in the Eurasian Zonal Circulation Index (EZCI, 1951-2017). The boxes represent the 25th–75th percentiles; the line through each box represents the median; the whiskers indicate the 90th and 10th percentiles; and the points above and below the whiskers indicate the 95th and 5th percentiles, respectively.

Appendix Fig. 5. Time series (1980-1983) of the $\delta^{18}O_P$ **at (A)** Amderma, **(B)** Arkhangelsk, **(C)** Kalinin, **(D)** Pechora, **(E)** Perm, **(F)** Riga, and **(G)** St. Petersburg and time series (1980-1983) of **(H)** the NAOI and **(I)** EZCI.

References

Aizen, V., Aizen, E., Melack, J., and Martma, T.: Isotopic measurements of precipitation on central Asian glaciers (Southeastern Tibet, northern Himalayas, central Tien Shan), J. Geophys. Res. Atmos., 101, 9185-9196, https://doi.org/10.1029/96JD00061, 1996.

Aizen, V. B., Aizen, E., Fujita, K., Nikitin, S. A., Kreutz, K. J., and Takeuchi, L. N.: Stable-isotope time series and precipitation origin from firn-core and snow samples, Altai glaciers, Siberia, J. Glaciol., 51, 637-654, https://doi.org/10.3189/172756505781829034, 2005.

Aragufis-Aragufis, L., Froehlich, K., and Rozanski, K.: Stable isotope composition of precipitation over southeast Asia, J. Geophys. Res. Atmos., 103, 28721-28742, https://doi.org/10.1029/98JD02582, 1998.

Baldini, L. M., McDermott, F., Foley, A. M., and Baldini, J. U. L.: Spatial variability in the European winter precipitation δ^{18}O-NAO relationship: Implications for reconstructing NAO-mode climate variability in the Holocene, Geophys. Res. Lett., 35, https://doi.org/10.1029/2007gl032027, 2008.

Bershaw, J., Penny, S. M., and Garzione, C. N.: Stable isotopes of modern water across the Himalaya and eastern Tibetan Plateau: Implications for estimates of paleoelevation and paleoclimate, J. Geophys. Res.Atmos., 117, https://doi.org/10.1029/2011JD016132, 2012.

Blyakharchuk, T. A., Wright, H. E., Borodavko, P. S., Knaap, W. O. V. D., and Ammann, B.: Late Glacial and Holocene vegetational history of the Altai Mountains (southwestern Tuva Republic, Siberia), Palaeogeogr. Palaeocl., 245, 518-534, https://doi.org/10.1016/j.palaeo.2006.09.010, 2007.

Butzin, M., Werner, M., Masson-Delmotte, V., Risi, C., Frankenberg, C., Gribanov, K., Jouzel, J., and Zakharov, V. I.: Variations of oxygen-18 in West Siberian precipitation during the last 50 years, Atmos. Chem. Phys., 14, 5853-5869, https://doi.org/10.5194/acp-14-5853-2014, 2014.

Casado, M., Ortega, P., Masson-Delmotte, V., Risi, C., Swingedouw, D., Daux, V., Genty, D., Maignan, F., Solomina, O., Vinther, B., Viovy, N., and Yiou, P.: Impact of precipitation intermittency on NAO-temperature signals in proxy records, Clim. Past., 9, 871-886, https://doi.org/10.5194/cp-9-871-2013, 2013.

Chen, F. L., Zhang, M. J., Wang, S. J., Ma, Q., Zhu, X. F., and Dong, L.: Relationship between sub-cloud secondary evaporation and stable isotopes in precipitation of Lanzhou and surrounding area, Quatern. Int., 380-381, 68-74, https://doi.org/10.1016/j.quaint.2014.12.051, 2015.

Cruz Jr, F. W., Karmann, I., Viana Jr, O., Burns, S. J., Ferrari, J. A., Vuille, M., Sial, A. N., and Moreira, M. Z.: Stable isotope study of cave percolation waters in subtropical Brazil: Implications for paleoclimate inferences from speleothems, Chem. Geol., 220, 245-262, https://doi.org/10.1016/j.chemgeo.2005.04.001, 2005.

Dansgaard, W.: Stable isotopes in precipitation, Tellus, 16, 436-468, https://doi.org/10.3402/tellusa.v16i4.8993, 1964.

Dobinski, W.: Permafrost, Earth-Sci. Rev., 108, 158-169, https://doi.org/10.1016/j.earscirev.2011.06.007, 2011.

Field, R. D.: Observed and modeled controls on precipitation $\delta^{18}O$ over Europe: From local temperature to the Northern Annular Mode, J. Geophys. Res., 115, https://doi.org/10.1029/2009jd013370, 2010.

Henderson, K., Laube, A., Gäggeler, H. W., Olivier, S., Papina, T., and Schwikowski, M.: Temporal variations of accumulation and temperature during the past two centuries from Belukha ice core, Siberian Altai, J. Geophys. Res., 111, https://doi.org/10.1029/2005jd005819, 2006.

Hoffmann, G. and Heimann, M.: Water isotope modeling in the Asian monsoon region, Quatern. Int., 37, 115-128, https://doi.org/10.1016/1040-6182(96)00004-3, 1997.

Hou, D. J., Qin, X., Wu, J. K., and Du, W. T.: Characteristics of stable isotopes in precipitation and the water vapor sources in Urumqi, Journal of Arid Land Resources and Environment, 25, 136-142, https://doi.org/10.13448/j.cnki.jalre.2011.10.026, 2011. (In Chinese with English abstract and figures)

Hoy, A., Sepp, M., and Matschullat, J.: Large-scale atmospheric circulation forms and their impact on air temperature in Europe and northern Asia, Theor. Appl. Climatol., 113, 643-658, https://doi.org/10.1007/s00704-012-0813-9, 2012.

Hurrell, J. W.: Decadal trends in the North Atlantic Oscillation: regional temperatures and precipitation, Science, 269, 676-679, https://doi.org/10.1126/science.269.5224.676, 1995.

Hurrell, J. W., Kushnir, Y., Ottersen, G., and Visbeck, M.: An overview of the North Atlantic Oscillation, in: The North Atlantic Oscillation: Climatic Significance and Environmental Impact, Geophysical Monograph 134, Copyright by the American Geophysical Union, American, https://doi.org/10.1029/134GM01, 2003.

Johnson, K. R. and Ingram, B. L.: Spatial and temporal variability in the stable isotope systematics of modern precipitation in China: implications for paleoclimate reconstructions, Earth. Planet. Sc. Lett., 220, 365-377, https://doi.org/10.1016/s0012-821x(04)00036-6, 2004.

Krklec, K. and Domínguez-Villar, D.: Quantification of the impact of moisture source regions on the oxygen isotope composition of precipitation over Eagle Cave, central Spain, Geochim. Cosmochim. Ac., 134, 39-54, https://doi.org/10.1016/j.gca.2014.03.011, 2014.

Krklec, K., Domínguez-Villar, D., and Lojen, S.: The impact of moisture sources on the oxygen isotope composition of precipitation at a continental site in central Europe, J. Hydrol., 561, 810-821, https://doi.org/10.1016/j.jhydrol.2018.04.045, 2018.

Kurita, N.: Relationship between the variation of isotopic ratios and the source of summer precipitation in eastern Siberia, J. Geophys. Res., 108, https://doi.org/10.1029/2001jd001359, 2003.

Kurita, N., Yoshida, N., Inoue, G., and Chayanova, E. A.: Modern isotope climatology of Russia: A first assessment, J. Geophys. Res.: Atmos., 109, https://doi.org/10.1029/2003jd003404, 2004.

Langebroek, P. M., Werner, M., and Lohmann, G.: Climate information imprinted in oxygen-isotopic composition of precipitation in Europe, Earth. Planet. Sc. Lett., 311, 144-154, https://doi.org/10.1016/j.epsl.2011.08.049, 2011.

Li, J. P. and Wang, J. X. L.: A modified zonal index and its physical sense, Geophys. Res. Lett., 30, https://doi.org/10.1029/2003gl017441, 2003.

Li, T.-Y.: False amounte effect - A discussion on issue of isotopic climatolog, Quaternary Science, 38, 1545-1548, https://doi.org/10.11928/j.issn.1001-7410.2018.06, 2018. (In Chinese with English figures)

Li, X.-F., Zhang, M.-J., Li, Y.-J., Wang, S.-J., Huang, X.-Y., Ma, Q., and Ma, X.-N.: Characteristics of $\delta^{18}O$ in Precipitation and Moisture Transports over the Arid Region in Northwest China, Environmental Science, 33, 711-719, https://doi.org/10.13227/j.hjkx.2012.03.010, 2012a. (In Chinese with English abstract and figures)

Li, X.-F., Zhang, M.-J., Ma, Q., Li, Y.-J., Wang, S.-J., and Wang, B.-L.: Characteristics of Stable Isotopes in Precipitation over Northeast China and Its Water Vapor Sources, Environmental Science, 33, 2924-2931, https://doi.org/10.13227/j.hjkx.2012.09.009, 2012b. (In Chinese with English abstract and figures)

Liu, X. K., Rao, Z. G., Zhang, X. J., Huang, W., Chen, J. H., and Chen, F. H.: Variations in the oxygen isotopic composition of precipitation in the Tianshan Mountains region and their significance for the Westerly circulation, J. Geogr. Sci., 25, 801-816, https://doi.org/10.1007/s11442-015-1203-x, 2015.

Mischel, S. A., Scholz, D., and Spötl, C.: $\delta^{18}O$ values of cave drip water: a promising proxy for the reconstruction of the North Atlantic Oscillation?, Clim. Dynam., 45, 3035-3050, https://doi.org/10.1007/s00382-015-2521-5, 2015.

Nowosad, M.: Variability of the zonal circulation index over Central Europe according to the Lityński method, Geographia Polonica, 90, 417-430, https://doi.org/10.7163/GPol.0111, 2017.

Numaguti, A.: Origin and recycling processes of precipitating water over the Eurasian continent: Experiments using an atmospheric general circulation model, J. Geophys. Res. Atmos., 104, 1957-1972, https://doi.org/10.1029/1998jd200026, 1999.

Pang, Z. H., Kong, Y. L., Froehlich, K., Huang, T. M., Yuan, L. J., Li, Z. Q., and Wang, F. T.: Processes affecting isotopes in precipitation of an arid region, Tellus. B., 63, 352-359, https://doi.org/10.1111/j.1600-0889.2011.00532.x, 2011.

Earth Syst. Dynam. Discuss., https://doi.org/10.5194/esd-2019-7
Manuscript under review for journal Earth Syst. Dynam.
Discussion started: 28 February 2019

Peng, H.-D., Mayer, B., Harris, S., and Krouse, H. R.: The influence of below-cloud secondary effects on the stable isotope composition of hydrogen and oxygen in precipitation at Calgary, Alberta, Canada, Tellus, 59, 698-704, https://doi.org/10.1111/j.1600-0889.2007.00291.x, 2007.

Peng, H.-D., Mayer, B., Norman, A.-L., and Krouse, H. R.: Modelling of hydrogen and oxygen isotope compositions for local precipitation, Tellus. B., 57, 273-282, https://doi.org/10.3402/tellusb.v57i4.16545, 2005.

Peng, S. and Mysak, L. A.: A teleconnection study of interannual sea surface temperature fluctuations in the northern North Atlantic and precipitation and runoff over Western Siberia, J. Climate., 6:5, 876-885, https://doi.org/10.1175/1520-0442(1993)006<0876:ATSOIS>2.0.CO;2, 1993.

Pfahl, S. and Sodemann, H.: What controls deuterium excess in global precipitation?, Clim. Past., 10, 771-781, https://doi.org/10.5194/cp-10-771-2014, 2014.

Pfahl, S. and Wernli, H.: Air parcel trajectory analysis of stable isotopes in water vapor in the eastern Mediterranean, J. Geophys. Res., 113, https://doi.org/10.1029/2008jd009839, 2008.

Raudina, T. V., Loiko, S. V., Lim, A., Manasypov, R. M., Shirokova, L. S., Istigechev, G. I., Kuzmina, D. M., Kulizhsky, S. P., Vorobyev, S. N., and Pokrovsky, O. S.: Permafrost thaw and climate warming may decrease the CO_2, carbon, and metal concentration in peat soil waters of the Western Siberia Lowland, Sci. Total. Environ., 634, 1004-1023, https://doi.org/10.1016/j.scitotenv.2018.04.059, 2018.

Rozanski, K., Araguás-Araguás, L., and Gonfiantini, R.: Relation between long-term trends of oxygen-18 isotope composition of precipitation and climate, Science, 258, 981-985, https://doi.org/10.1126/science.258.5084.981, 1992.

Rozanski, K., Araguas-Araguas, L., and Gonfiantini, R.: Isotopic Patterns in Modern Global Precipitation, In: Climate Change in Continental Isotopic Records, edited by: Swart, P. K., Lohmann, K. C., Mckenzie, J., and Savin, S., Geophys.Monogr., 78: 1-36, https://doi.org/10.1029/GM078p0001, 1993.

Schuur, E. A., McGuire, A. D., Schadel, C., Grosse, G., Harden, J. W., Hayes, D. J., Hugelius, G., Koven, C. D., Kuhry, P., Lawrence, D. M., Natali, S. M., Olefeldt, D., Romanovsky, V. E., Schaefer, K., Turetsky, M. R., Treat, C. C., and Vonk, J. E.: Climate change and the permafrost carbon feedback, Nature, 520, 171-179, https://doi.org/10.1038/nature14338, 2015.

Sidorova, O. V., Siegwolf, R. T. W., Saurer, M., Naurzbaev, M. M., Shashkin, A. V., and Vaganov, E. A.: Spatial patterns of climatic changes in the Eurasian north reflected in Siberian larch tree-ring parameters and stable isotopes, Global. Change. Biol., 16, 1003-1018, https://doi.org/10.1111/j.1365-2486.2009.02008.x, 2010.

Stewart, M. K.: Stable isotope fractionation due to evaporation and isotopic exchange of falling waterdrops: Applications to atmospheric processes and evaporation of lakes, J. Geophys. Res., 80, 1133-1146, https://doi.org/10.1029/JC080i009p01133, 1975.

Tang, Y., Pang, H., Zhang, W., Li, Y., Wu, S., and Hou, S.: Effects of changes in moisture source and the upstream rainout on stable isotopes in summer precipitation – a case study in Nanjing, East China, Hydrol. Earth. Syst. Sc., 12, 3919-3944, https://doi.org/10.5194/hess-19-4293-2015, 2015.

Tian, L. D., Yao, T. D., MacClune, K., White, J. W. C., Schilla, A., Vaughn, B., Vachon, R., and Ichiyanagi, K.: Stable isotopic variations in west China: A consideration of moisture sources, J. Geophys. Res. Atmos, 112, https://doi.org/10.1029/2006jd007718, 2007.

Wang, S. J., Zhang, M. J., Crawford, J., Hughes, C. E., Du, M. X., and Liu, X. M.: The effect of moisture source and synoptic conditions on precipitation isotopes in arid central Asia, J. Geophys. Res.Atmos., 122, 2667-2682, https://doi.org/10.1002/2015jd024626, 2017.

Wang, S. J., Zhang, M. J., Hughes, C. E., Zhu, X. F., Dong, L., Ren, Z. G., and Chen, F. L.: Factors controlling stable isotope composition of precipitation in arid conditions: an observation network in the Tianshan Mountains, central Asia, Tellus. B., 68(sup1), 289-299, https://doi.org/10.3402/tellusb.v68.26206, 2016.

Wang, Y. J., Cheng, H., Edwards, R. L., An, Z. S., Wu, J. Y., Shen, C. C., and Dorale, J. A.: A high-resolution absolute-dated late Pleistocene Monsoon record from Hulu Cave, China, Science, 294, 2345-2348, https://doi.org/10.1126/science.1064618, 2001.

Wassenburg, J. A., Dietrich, S., Fietzke, J., Fohlmeister, J., Jochum, K. P., Scholz, D., Richter, D. K., Sabaoui, A., Spötl, C., Lohmann, G., Andreae, Meinrat O., and Immenhauser, A.: Reorganization of the North Atlantic Oscillation during early Holocene deglaciation, Nat. Geosci., 9, 602-605, https://doi.org/10.1038/ngeo2767, 2016.

Wolff, C., Plessen, B., Dudashvilli, A. S., Breitenbach, S. F. M., Cheng, H., Edwards, L. R., and Strecker, M. R.: Precipitation evolution of Central Asia during the last 5000 years, The Holocene., 27, 142-

154, https://doi.org/10.1177/0959683616652711, 2016.

Yamanaka, T., Tsujimura, M., Oyunbaatar, D., and Davaa, G.: Isotopic variation of precipitation over eastern Mongolia and its implication for the atmospheric water cycle, J. Hydrol., 333, 21-34, https://doi.org/10.1016/j.jhydrol.2006.07.022, 2007.

Yu, W. S., Tian, L. D., Risi, C., Yao, T. D., Ma, Y. M., Zhao, H. B., Zhu, H. F., He, Y., Xu, B. Q., Zhang, H. B., and Qu, D. M.: $\delta^{18}O$ records in water vapor and an ice core from the eastern Pamir Plateau: Implications for paleoclimate reconstructions, Earth. Planet. Sc. Lett., 456, 146-156, https://doi.org/10.1016/j.epsl.2016.10.001, 2016.

Zhang, J. and Li, T.-Y.: "Amount effect" vs. "Circulation effect":The climate significance of precipitation and stalagmit $\delta^{18}O$ in the Asian-Australian monsoon region over the past 1 ka, Quaternary Science, 38, 1532-1544, https://doi.org/10.11928/j.issn.1001-7410.2018.06.19, 2018. (In Chinese with English abstract and figures)

Zhang, X.-W.: Vertical Distribution of the Transported Quantity of Material and Energy by Airflow, Desert and Oasis Meteorology, 3, 1-5, 2009. (In Chinese with English abstract and figures)

Zhao, H. B., Xu, B. Q., Yao, T. D., Wu, G. J., Lin, S. B., Gao, J., and Wang, M.: Deuterium excess record in a southern Tibetan ice core and its potential climatic implications, Clim. Dynam., 38, 1791-1803, https://doi.org/10.1007/s00382-011-1161-7, 2011.

Earth Syst. Dynam. Discuss., https://doi.org/10.5194/esd-2019-7
Manuscript under review for journal Earth Syst. Dynam.
Discussion started: 28 February 2019

Earth System Dynamics
Discussions

Fig. 1

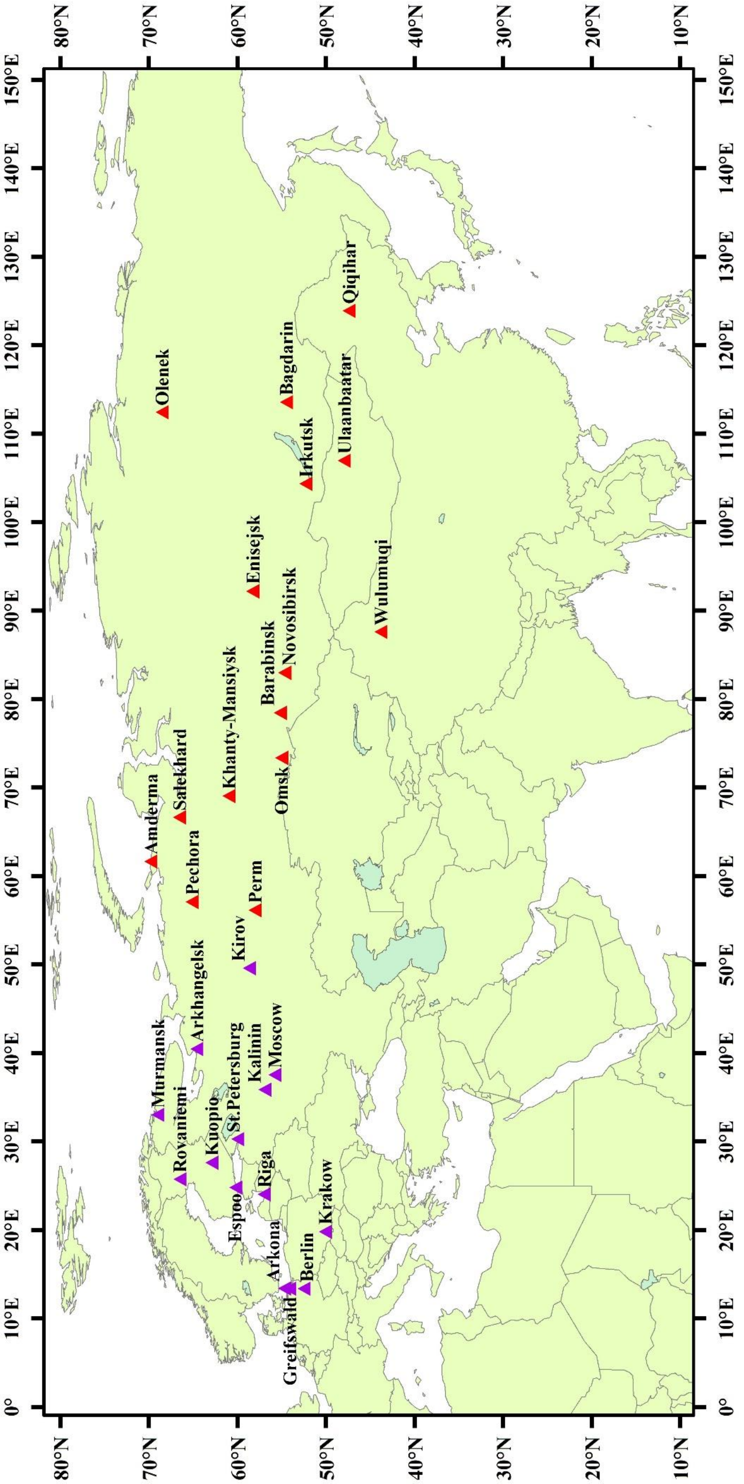

742 **Fig. 2**

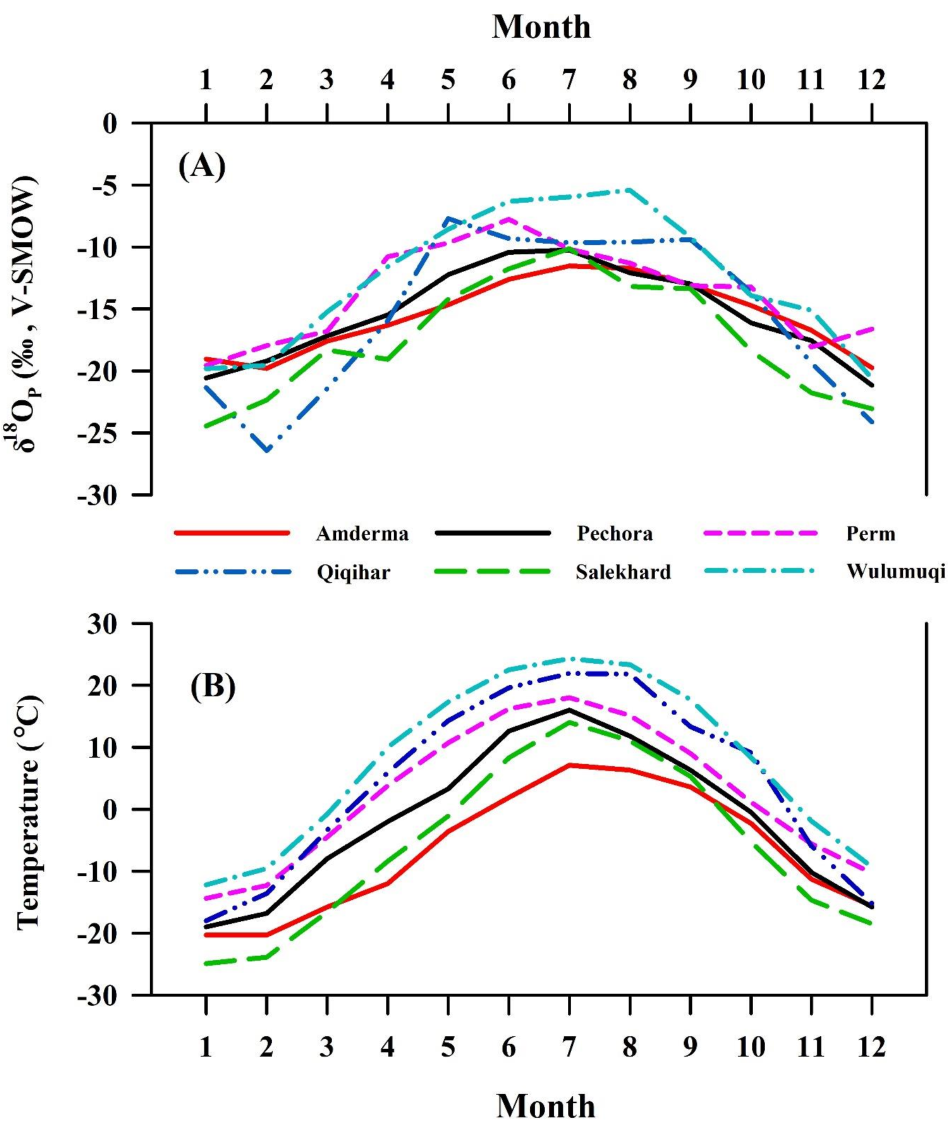

743

744

745

746

747

Earth Syst. Dynam. Discuss., https://doi.org/10.5194/esd-2019-7
Manuscript under review for journal Earth Syst. Dynam.
Discussion started: 28 February 2019

Earth System Dynamics
Open Access
Discussions

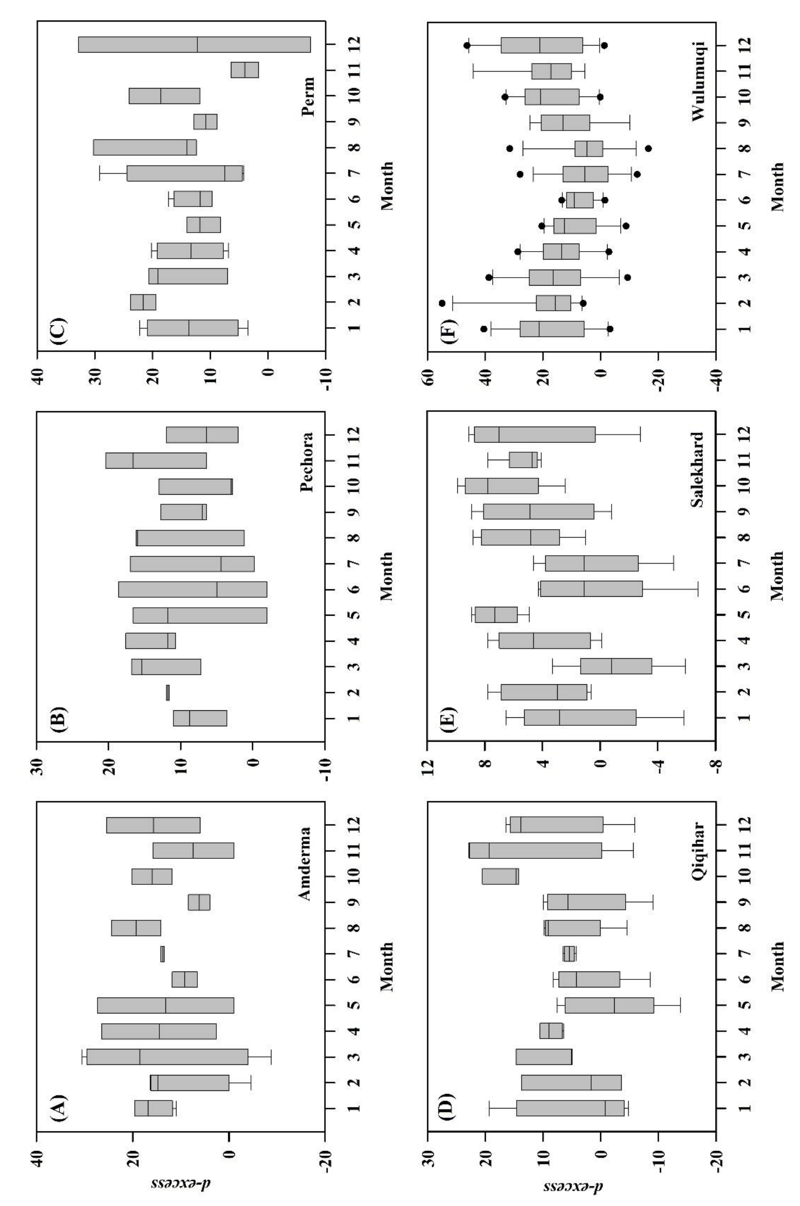

Fig. 3

Fig. 4

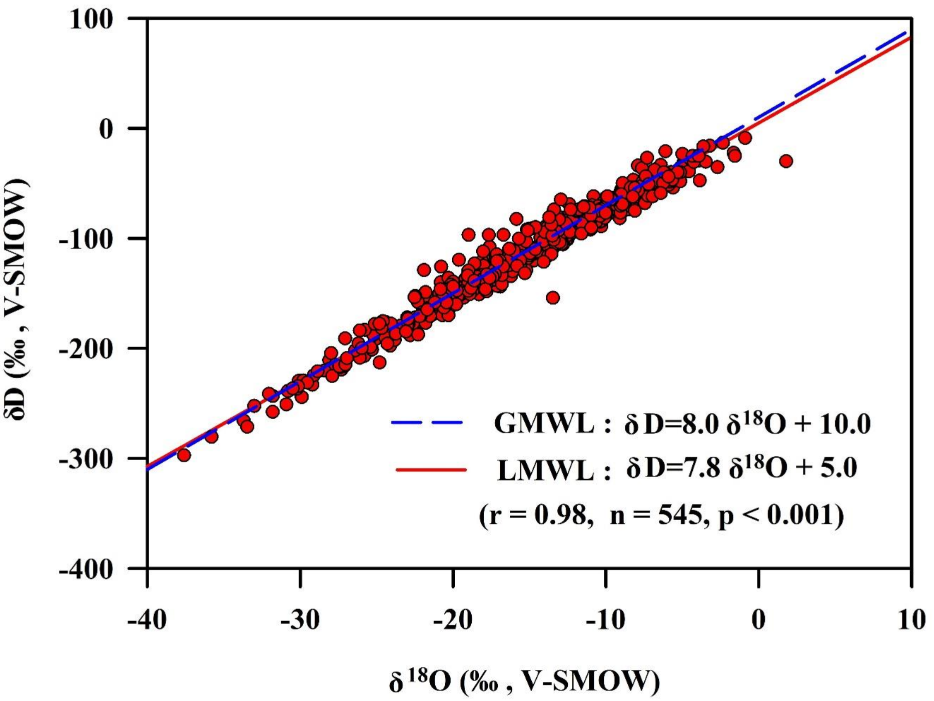
100
0
-100
-200
-300
-400
δD (‰ , V-SMOW)
-40
-30
-20
-10
0
10
δ18O (‰ , V-SMOW)
GMWL : δD=8.0 δ18O + 10.0
LMWL : δD=7.8 δ18O + 5.0
(r = 0.98, n = 545, p < 0.001)

Earth Syst. Dynam. Discuss., https://doi.org/10.5194/esd-2019-7
Manuscript under review for journal Earth Syst. Dynam.
Discussion started: 28 February 2019

Earth System Dynamics
Discussions
Open Access

Fig. 5

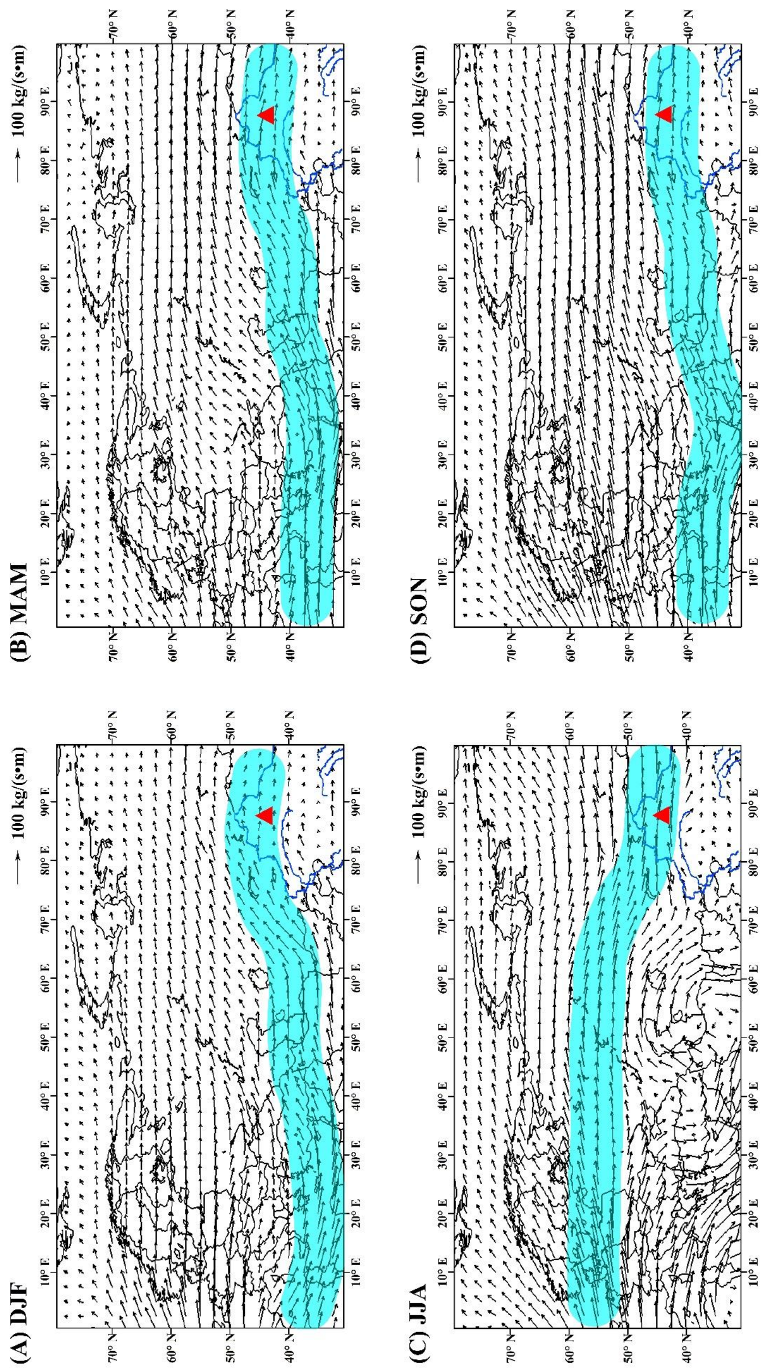

Earth Syst. Dynam. Discuss., https://doi.org/10.5194/esd-2019-7
Manuscript under review for journal Earth Syst. Dynam.
Discussion started: 28 February 2019

Earth System Dynamics
Discussions

Fig. 6

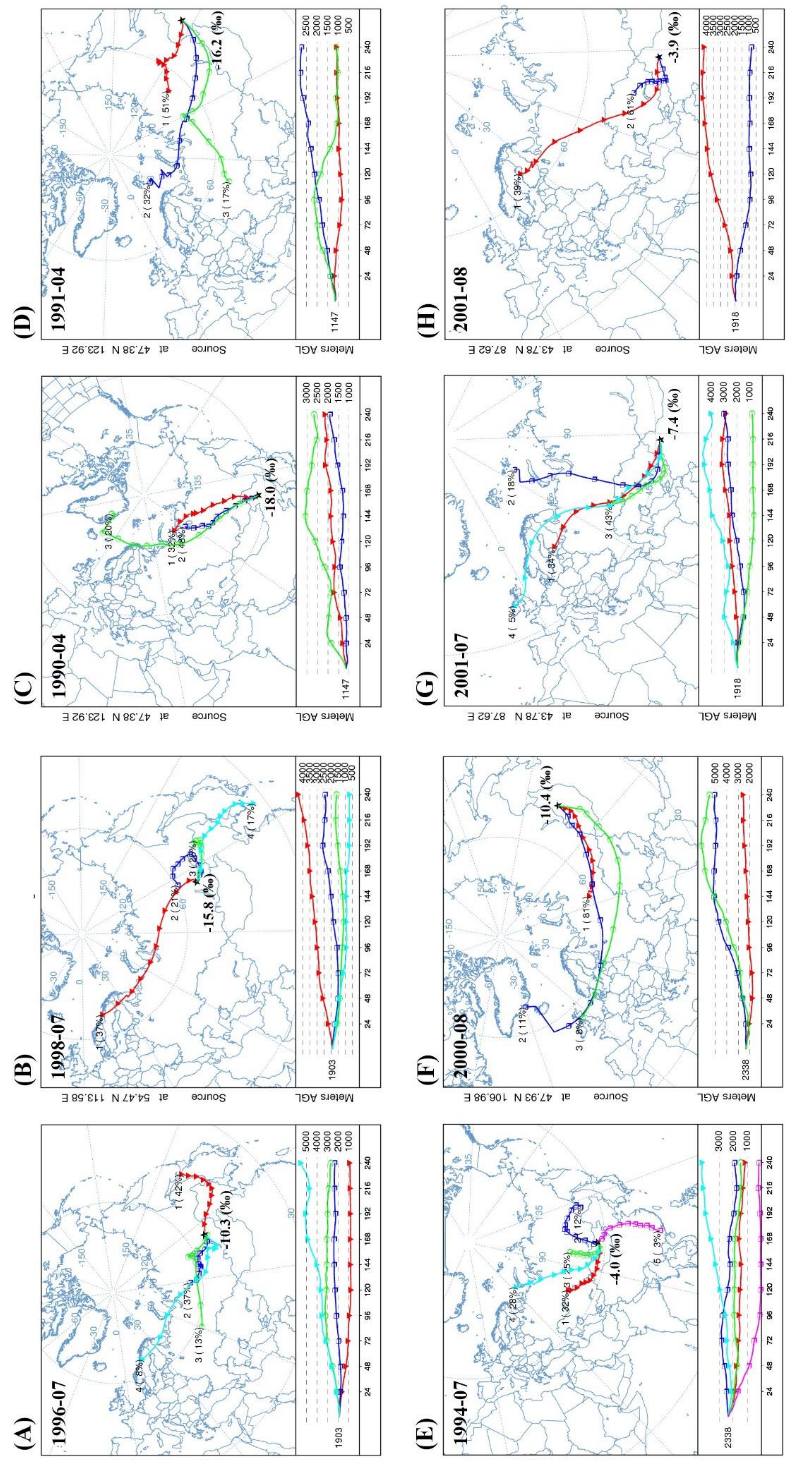

Earth Syst. Dynam. Discuss., https://doi.org/10.5194/esd-2019-7
Manuscript under review for journal Earth Syst. Dynam.
Discussion started: 28 February 2019

Fig. 7

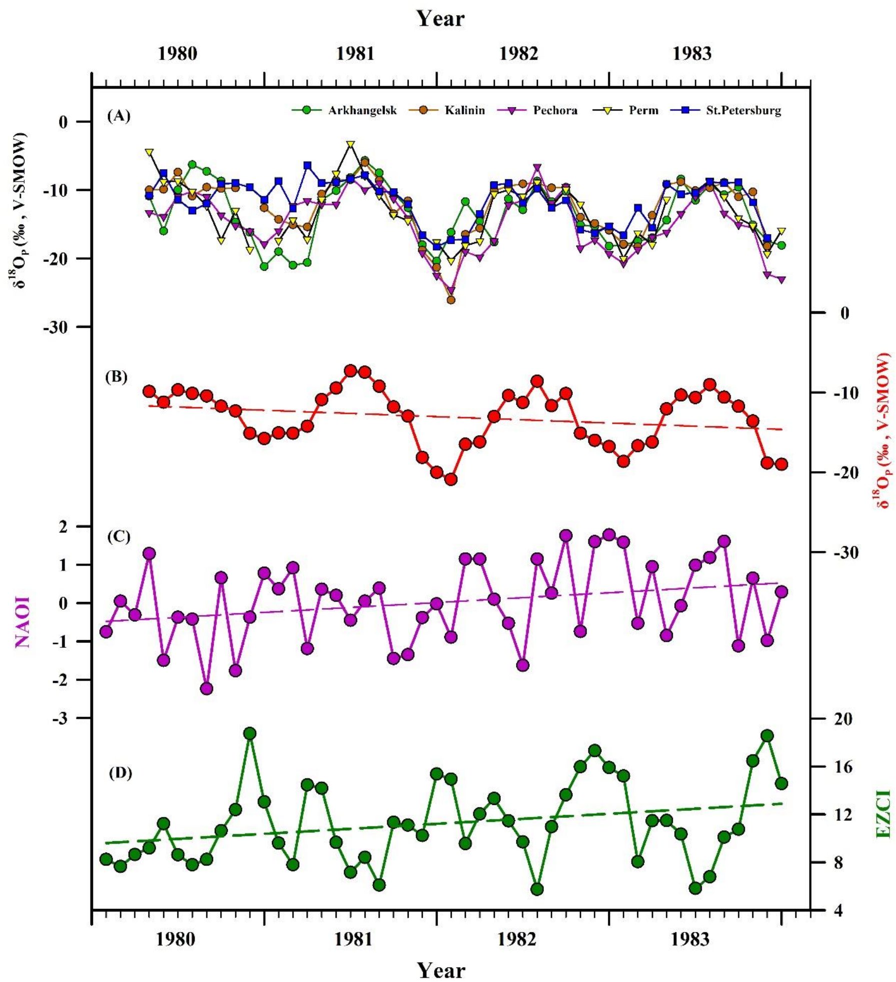

Earth Syst. Dynam. Discuss., https://doi.org/10.5194/esd-2019-7
Manuscript under review for journal Earth Syst. Dynam.
Discussion started: 28 February 2019

Earth System Dynamics
Discussions

Fig. 8

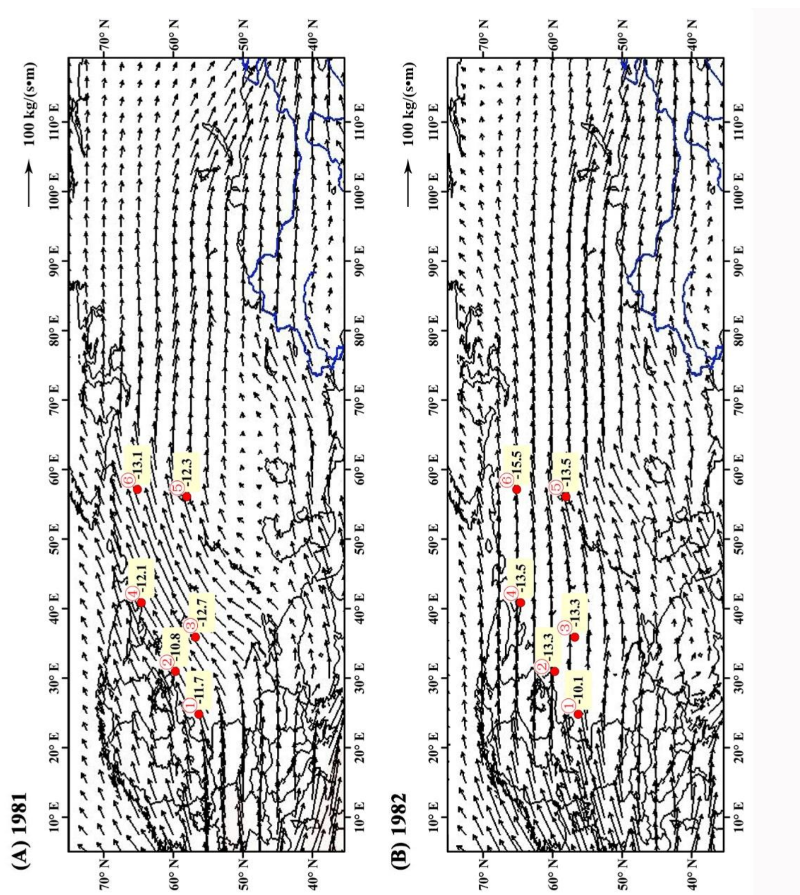

Earth Syst. Dynam. Discuss., https://doi.org/10.5194/esd-2019-7
Manuscript under review for journal Earth Syst. Dynam.
Discussion started: 28 February 2019

Table 1 GNIP stations in Siberia and Central Asia considered in this study. For each station, we report the annual precipitation; annual average temperature; weighted average annual $\delta^{18}O$, δD and *d-excess* values in precipitation ($\delta^{18}O_W$, δD_W, and *d-excess$_{(W)}$*); latitude; longitude; and altitude, as well as the monitoring period and the number of available monthly measurements (n).

Site	Latitude (°N)	Longitude (°E)	Altitude (m)	Annual precipitation (mm)	$\delta^{18}O_W$ (‰, V-SMOW)	δD_W (‰, V-SMOW)	*d-excess$_{(W)}$*	Annual average temperature (℃)	Monitoring year (A.D)	n
Amderma	69.77	61.68	53	443	-15.5	-110.1	14.4	-7.0	1980-1990	31
Bagdarin	54.47	113.58	903	438	-13.7	-106.6	2.7	-5.3	1996-2000	34
Barabinsk	55.33	78.37	120	371	-12.4	-96.4	2.5	1.1	1996-2000	28
Enisejsk	58.45	92.15	78	491	-13.3	-98.4	7.9	-1.5	1990	12
Irkutsk	52.27	104.35	485	445	-12.4	-97.3	2.2	0.0	1971-1990	14
Khanty-Mansiysk	60.97	69.07	40	563	-11.6	-92.5	0.4	-1.3	1996-1997	13
Novosibirsk	55.03	82.90	162	422	-14.6	-104.3	12.8	0.9	1990	12
Olenek	68.50	112.43	220	300	-18.7	-145.5	3.8	-11.8	1996-2000	36
Omsk	55.01	73.38	94	401	-13.5	-98.2	8.9	1.6	1990	8
Pechora	65.12	57.10	56	578	-15.0	-109.5	9.2	-1.8	1980-1990	36
Perm	58.01	56.18	161	616	-12.5	-92.1	13.9	2.1	1980-1991	38
Qiqihar	47.38	123.92	147	581	-10.6	-79.1	5.5	4.3	1988-1992	50
Salekhard	66.53	66.67	16	446	-16.5	-127.7	4.5	-6.2	1996-2000	58
Ulaanbaatar	47.93	106.98	1338	249	-8.5	-64.8	2.9	-0.3	1998-2001	44
Wulumuqi	43.78	87.62	918	303	-10.6	-72.2	12.5	7.5	1986-2003	131

Earth Syst. Dynam. Discuss., https://doi.org/10.5194/esd-2019-7
Manuscript under review for journal Earth Syst. Dynam.
Discussion started: 28 February 2019

Table 2 LMWL of 15 studied GNIP sites in Siberia and Central Asia and the number of available monthly measurements (n)

Site	LMWL	n
Amderma	$\delta D = 7.62\ \delta^{18}O + 6.86$	31
Bagdarin	$\delta D = 7.84\ \delta^{18}O - 0.18$	34
Barabinsk	$\delta D = 7.43\ \delta^{18}O - 6.01$	28
Enisejsk	$\delta D = 8.68\ \delta^{18}O + 16.53$	12
Irkutsk	$\delta D = 8.05\ \delta^{18}O + 6.78$	14
Khanty-Mansiysk	$\delta D = 7.98\ \delta^{18}O - 0.02$	13
Novosibirsk	$\delta D = 8.77\ \delta^{18}O + 24.1$	12
Olenek	$\delta D = 7.77\ \delta^{18}O - 2.94$	36
Omsk	$\delta D = 7.61\ \delta^{18}O + 1.95$	8
Pechora	$\delta D = 7.89\ \delta^{18}O + 8.14$	36
Perm	$\delta D = 8.00\ \delta^{18}O + 13.43$	38
Qiqihar	$\delta D = 7.59\ \delta^{18}O - 0.14$	50
Salekhard	$\delta D = 7.86\ \delta^{18}O + 1.21$	58
Ulaanbaatar	$\delta D = 7.82\ \delta^{18}O + 1.52$	44
Wulumuqi	$\delta D = 6.98\ \delta^{18}O + 0.43$	131

Earth Syst. Dynam. Discuss., https://doi.org/10.5194/esd-2019-7
Manuscript under review for journal Earth Syst. Dynam.
Discussion started: 28 February 2019

Earth System Dynamics Discussions Open Access

Table 3. Correlation coefficients between $\delta^{18}O_P$ and temperature based on monthly data (R_T)

Site	DJF	MAM	JJA	SON	ALL	n
Amderma	0.32	0.49*	0.08	0.62**	0.75**	72
Bagdarin	——	0.82*	0.17	0.92**	0.90**	34
Barabinsk	0.49	0.96**	0.70	0.97**	0.96**	28
Enisejsk	——	——	——	——	0.88**	12
Khanty-Mansiysk	——	——	——	——	0.94**	13
Novosibirsk	——	——	——	——	0.88**	12
Olenek	0.69*	0.91**	0.12	0.77	0.94**	35
Pechora	0.50*	0.57**	0.55*	0.64**	0.85**	79
Perm	0.49*	0.79**	0.31	0.42	0.79**	79
Qiqihar	0.51	0.75**	0.17	0.46	0.76**	50
Salekhard	0.04	0.72**	0.54*	0.90**	0.88**	58
Ulaanbaatar	0.41	0.89*	0.10	0.93**	0.84**	44
Wulumuqi	——	0.71**	0.08	0.67**	0.86**	123

* Denotes a statistically significant relationship at $p<0.05$.
** Denotes a statistically significant relationship at $p<0.01$.
DJF: December-January-February; MAM: March-April-May; JJA: June-July-August; SON: September-October-November; All: the entire year

Earth Syst. Dynam. Discuss., https://doi.org/10.5194/esd-2019-7
Manuscript under review for journal Earth Syst. Dynam.
Discussion started: 28 February 2019

Earth System Dynamics
Open Access
Discussions

Table 4 Correlation coefficients between the annual mean temperature, annual precipitation, annual mean NAOI and $\delta^{18}O_W$ (R_T, R_P, and R_N)

Site	Latitude (°N)	Longitude (°E)	Altitude (m)	R_T	R_P	R_N	Years	n
Amderma	69.77	61.68	53	0.31	-0.37	-0.64	1980-1990	5
Arkhangelsk	64.58	40.50	13	0.70	0.35	0.00	1980-1986	7
Arkona	54.68	13.43	42	-0.02	-0.62	-0.26	1998-2007	10
Berlin	52.47	13.40	48	0.33	-0.16	-0.05	1978-2012	35
Espoo	60.18	24.83	30	**0.67****	0.14	**0.52***	2001-2015	15
Greifswald	54.10	13.41	2	0.25	0.01	0.15	2003-2013	11
Kalinin	56.90	35.90	31	-0.03	-0.02	0.56	1881/1988	7
Kirov	58.65	49.62	164	0.50	-0.52	0.05	1980/2000	9
Krakow	50.06	19.85	205	**0.43****	-0.12	0.25	1975-2016	42
Kuopio	62.89	27.63	116	**0.73***	0.45	**0.62***	2005-2015	11
Moscow	55.75	37.57	157	0.43	-0.38	-0.07	1970/1979	6
Murmansk	68.97	33.05	46	0.23	0.47	**0.73***	1980/1990	8
Pechora	65.12	57.10	56	0.61	-0.43	**-0.89***	1980-1990	6
Perm	58.01	56.18	161	-0.56	-0.02	-0.46	1980-1990	5
Qiqihar	47.38	123.92	147	-0.63	-0.47	0.50	1988-1992	5
Riga	56.97	24.07	3	-0.05	-0.10	0.06	1980-1988	8
Rovaniemi	66.50	25.76	107	0.14	0.60	0.44	2004-2014	11
Salekhard	66.53	66.67	16	**0.95***	-0.21	0.51	1996-2000	5
St. Petersburg	59.97	30.30	4	0.27	-0.04	0.13	1980-1989	9
Wulumuqi	43.78	87.62	918	-0.29	0.27	-0.36	1986-2003	12

* Denotes a statistically significant relationship at $p < 0.05$.
** Denotes a statistically significant relationship at $p < 0.01$.

Earth Syst. Dynam. Discuss., https://doi.org/10.5194/esd-2019-7
Manuscript under review for journal Earth Syst. Dynam.
Discussion started: 28 February 2019

Earth System Dynamics Discussions
Open Access

Table 5 Correlation coefficients between $\delta^{18}O_P$ and the rainfall amount based on monthly data (R_P)

Site	DJF	MAM	JJA	SON	ALL	n
Amderma	0.13	-0.30	-0.16	-0.05	-0.01	72
Bagdarin	——	0.42	-0.33	0.38	0.48**	34
Barabinsk	-0.20	0.23	0.02	0.41	0.35	28
Enisejsk	——	——	——	——	0.59*	12
Khanty-Mansiysk	——	——	——	——	0.88**	13
Novosibirsk	——	——	——	——	0.40	12
Olenek	-0.19	0.54	0.02	0.14	0.60**	36
Pechora	-0.21	0.13	-0.13	-0.37	0.19	79
Perm	-0.09	-0.15	-0.35	0.55*	0.15	79
Qiqihar	-0.25	0.16	-0.11	0.48	0.47**	50
Salekhard	-0.32	-0.11	-0.29	0.05	0.30*	58
Ulaanbaatar	0.49	0.46	-0.21	0.70*	0.63**	25
Wulumuqi	-0.02	0.03	-0.30	0.10	0.34**	123

* Denotes a statistically significant relationship at $p < 0.05$.

** Denotes a statistically significant relationship at $p < 0.01$.

DJF: December-January-February; MAM: March-April-May; JJA: June-July-August; SON: September-October-November; All: the entire year

Earth Syst. Dynam. Discuss., https://doi.org/10.5194/esd-2019-7
Manuscript under review for journal Earth Syst. Dynam.
Discussion started: 28 February 2019

Table 6 Correlation coefficients between $\delta^{18}O_P$ and the EZCI based on monthly data (R_Z)

Site	DJF	MAM	JJA	SON	ALL	n
Amderma	0.09	-0.55*	0.27	-0.43	-0.37**	74
Bagdarin	——	0.07	0.19	-0.04	-0.50**	34
Barabinsk	0.74*	-0.33	-0.41	0.87*	-0.50**	28
Enisejsk	——	——	——	——	-0.53	12
Khanty-Mansiysk	——	——	——	——	-0.41	13
Novosibirsk	——	——	——	——	-0.56	12
Olenek	0.20	-0.46	-0.13	-0.74	-0.70**	36
Pechora	-0.52*	-0.03	-0.55*	-0.41	-0.59**	79
Perm	0.18	-0.43	0.15	-0.40	-0.37**	79
Qiqihar	0.17	-0.13	-0.10	-0.62*	-0.44**	50
Salekhard	0.11	-0.36	-0.45	-0.34	-0.54**	58
Ulaanbaatar	-0.42	0.39	0.12	0.36	-0.19	26
Wulumuqi	0.06	0.11	0.12	-0.42*	-0.51**	131

* Denotes a statistically significant relationship at $p < 0.05$.
** Denotes a statistically significant relationship at $p < 0.01$.
DJF: December-January-February; MAM: March-April-May; JJA: June-July-August; SON: September-October-November; All: the entire year.

Earth Syst. Dynam. Discuss., https://doi.org/10.5194/esd-2019-7
Manuscript under review for journal Earth Syst. Dynam.
Discussion started: 28 February 2019

Earth System Dynamics
Open Access
Discussions

Appendix Fig. 1

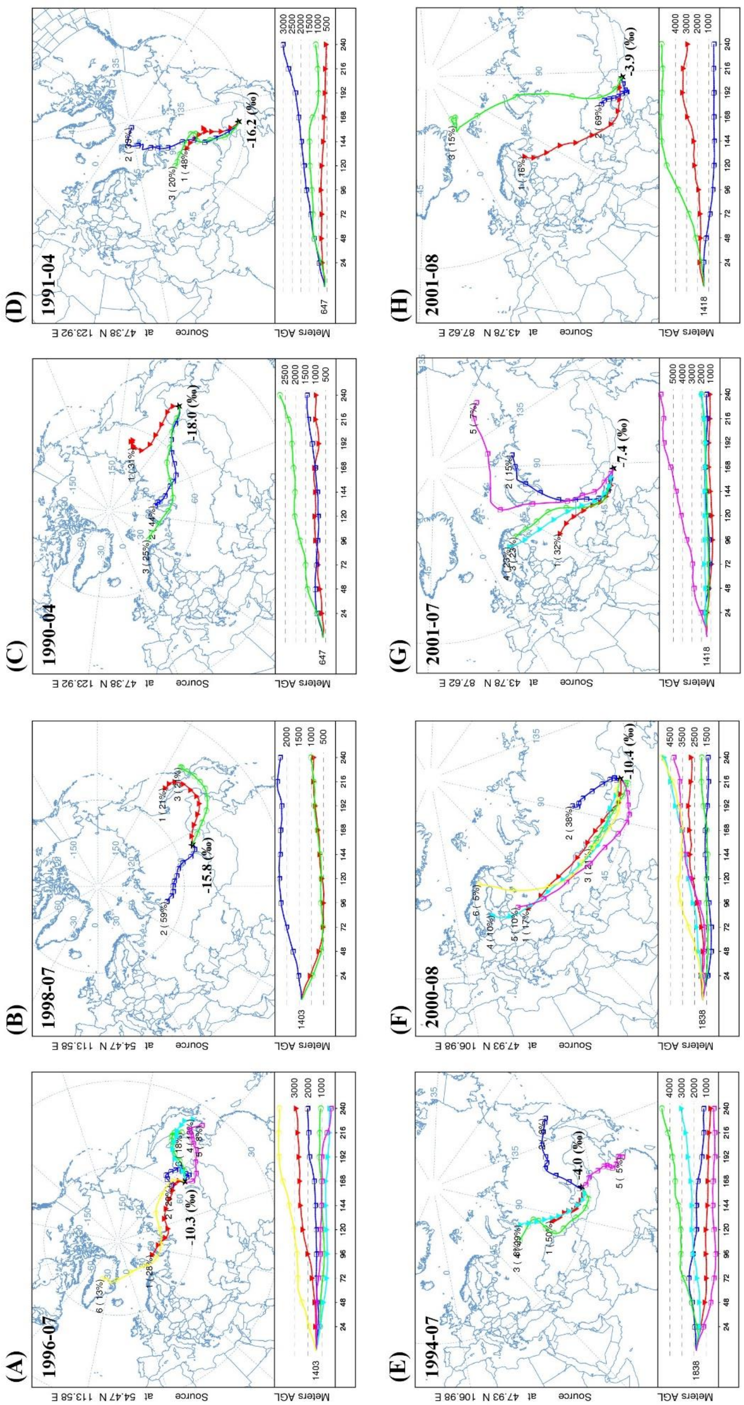

Earth Syst. Dynam. Discuss., https://doi.org/10.5194/esd-2019-7
Manuscript under review for journal Earth Syst. Dynam.
Discussion started: 28 February 2019

Earth System Dynamics
Discussions
Open Access

Appendix Fig. 2

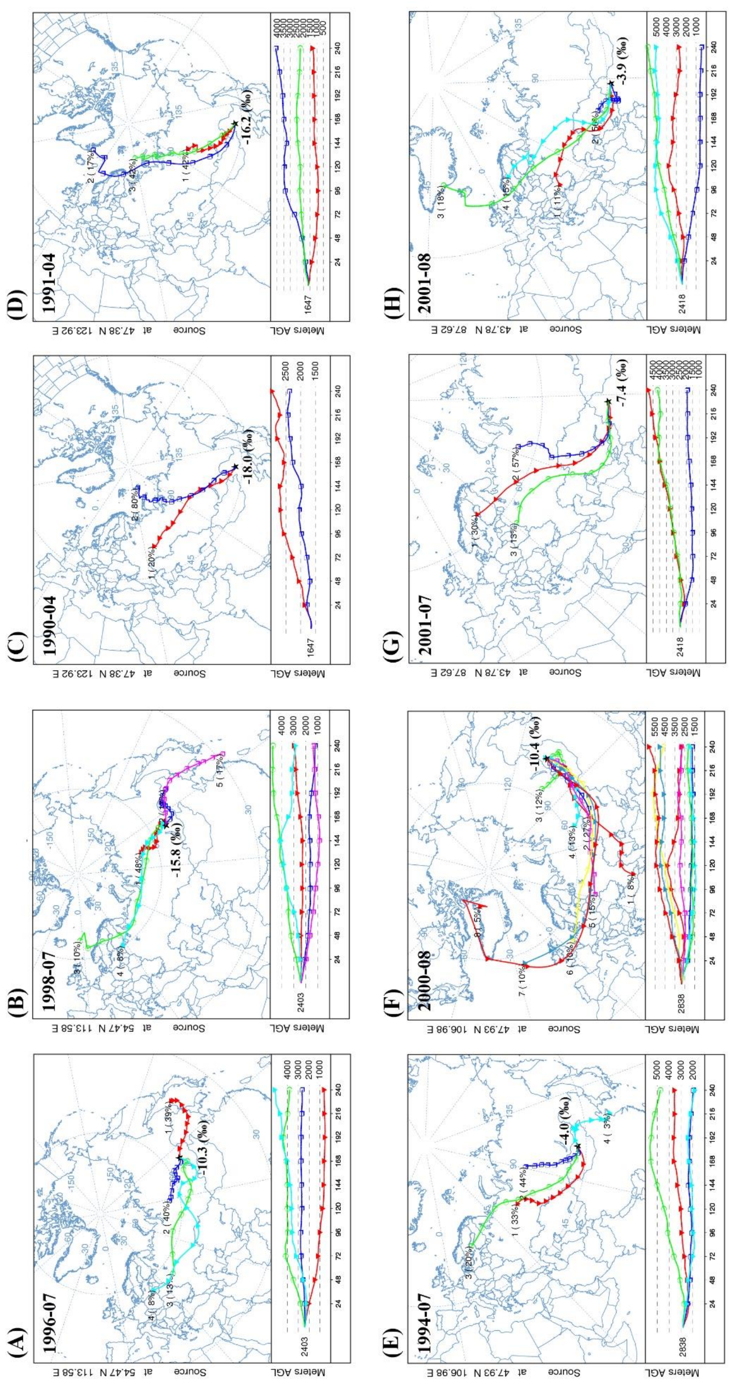

Earth Syst. Dynam. Discuss., https://doi.org/10.5194/esd-2019-7
Manuscript under review for journal Earth Syst. Dynam.
Discussion started: 28 February 2019

Earth System Dynamics
Discussions

Appendix Fig. 3

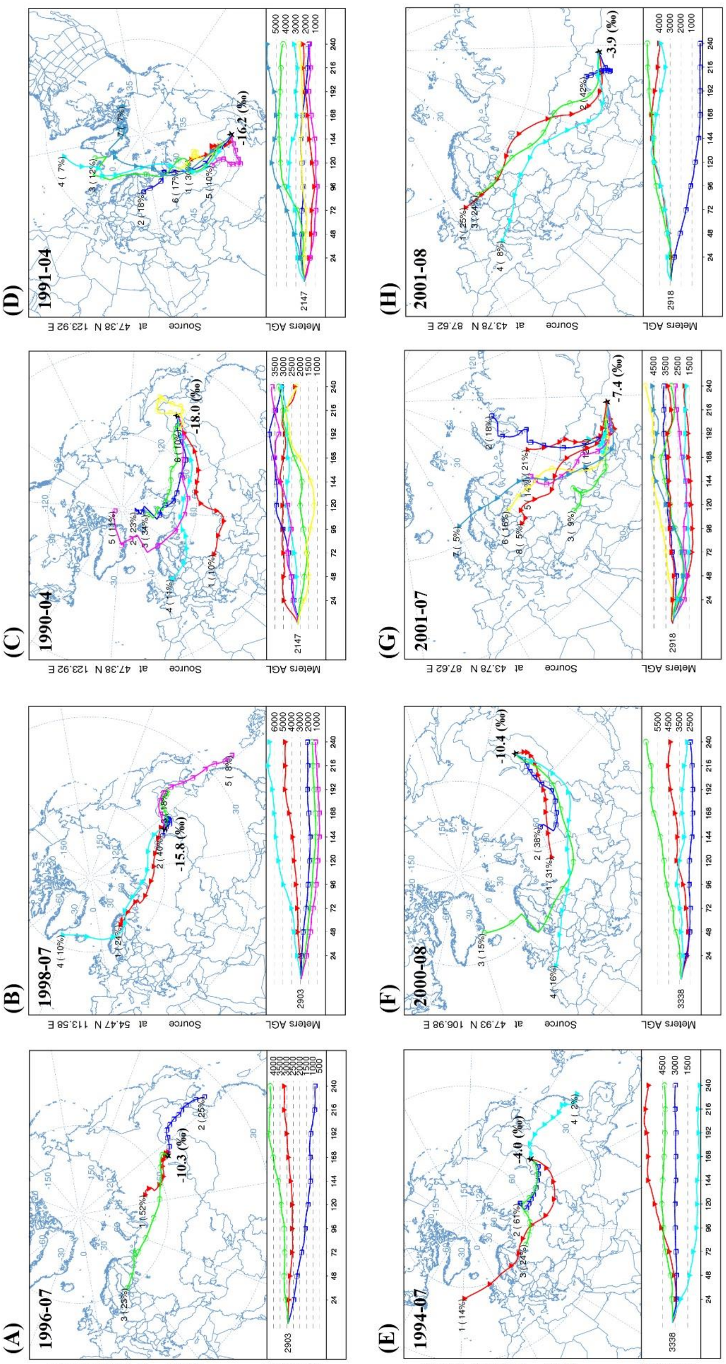

Appendix Fig. 4

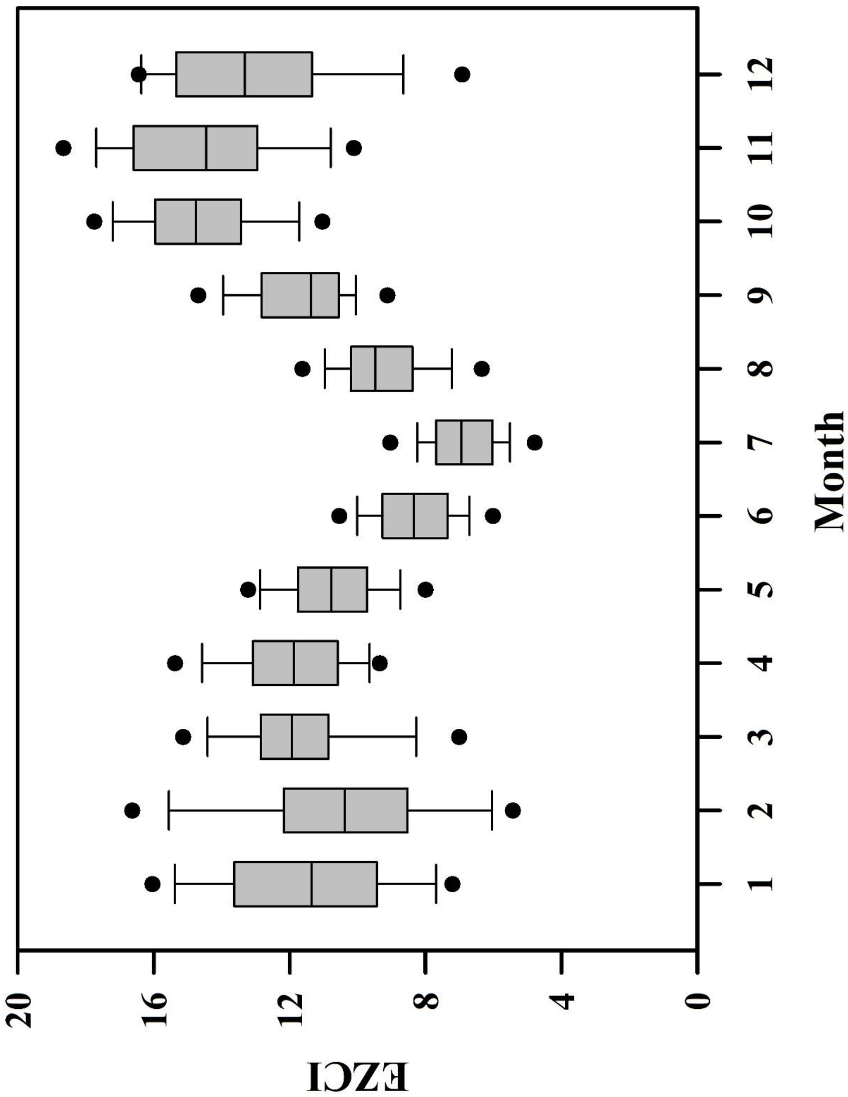

Earth Syst. Dynam. Discuss., https://doi.org/10.5194/esd-2019-7
Manuscript under review for journal Earth Syst. Dynam.
Discussion started: 28 February 2019

Earth System Dynamics
Discussions

Appendix Fig. 5

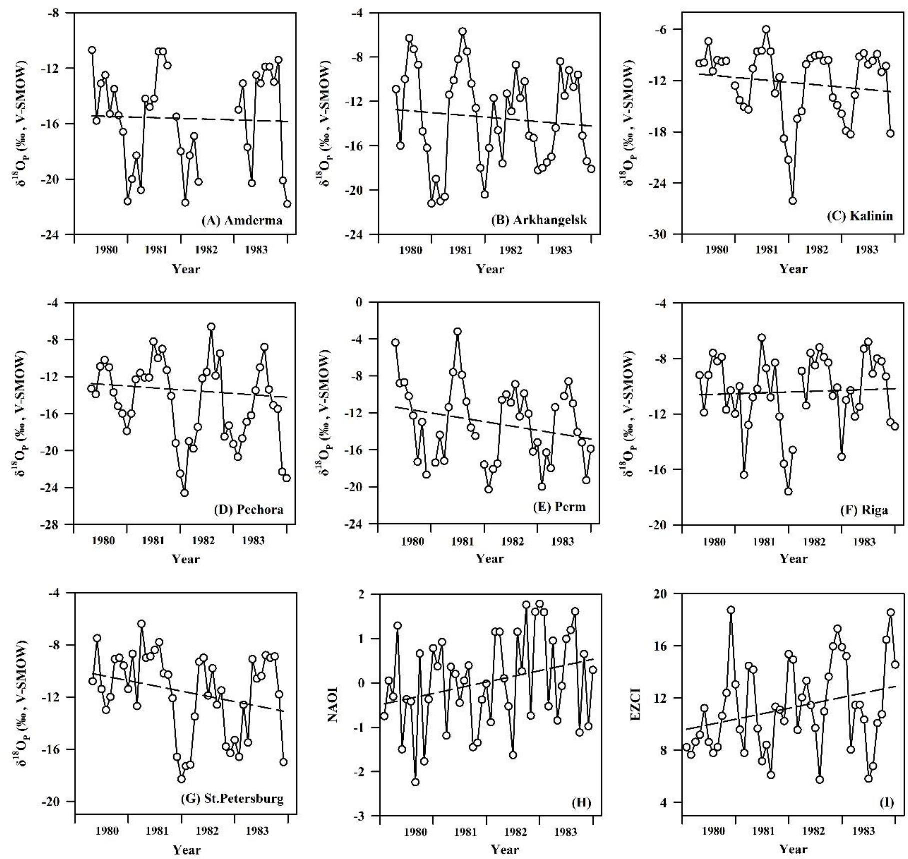

Appendix Table 1 Correlation coefficients between the temperature and rainfall amount based on monthly data (R_{TP})

Site	$R_{(TP)}$	n
Amderma	0.20*	122
Bagdarin	0.67**	55
Barabinsk	0.34**	60
Enisejsk	0.47**	128
Khanty-Mansiysk	0.49**	60
Novosibirsk	0.67*	12
Olenek	0.62**	59
Pechora	0.38**	129
Perm	0.30**	209
Qiqihar	0.66**	52
Salekhard	0.58**	191
Ulaanbaatar	0.59**	114
Wulumuqi	0.41**	152

* Denotes a statistically significant relationship at $p < 0.05$.
** Denotes a statistically significant relationship at $p < 0.01$.